THESIS FOR THE DEGREE OF LICENTIATE OF ENGINEERING

Energy Management for Vehicle–Home–Grid Systems

Degradation-Aware Online Control for Residential Bidirectional Charging

FRANCESCO POPOLIZIO

Department of Electrical Engineering
CHALMERS UNIVERSITY OF TECHNOLOGY
Gothenburg, Sweden, 2026

Energy Management for Vehicle–Home–Grid Systems
Degradation-Aware Online Control for Residential Bidirectional Charging

Francesco Popolizio

Acknowledgements, dedications, and similar personal statements in this thesis, reflect the author's own views.

Department of Electrical Engineering
Chalmers University of Technology
SE-412 96 Gothenburg, Sweden
Phone: +46 (0)31 772 1000

Cover:
Illustrative representation of a residential vehicle–home–grid system with rooftop photovoltaic (PV) generation, bidirectional EV charging, and electric grid connection. Created with the assistance of a generative AI tool and edited by the author.

Printed by Chalmers Digital Printing
Gothenburg, Sweden, March 2026

Energy Management for Vehicle–Home–Grid Systems
Degradation-Aware Online Control for Residential Bidirectional Charging
Francesco Popolizio
Department of Electrical Engineering
Chalmers University of Technology

Abstract

Electric vehicles (EVs) are rapidly becoming a mainstream transport technology, and their growing diffusion is influencing mobility and electricity systems. Since most cars are parked for most of the day, their idle time can offer an opportunity to provide flexibility. When equipped with bidirectional charging capability, an EV can support vehicle-to-home (V2H) operation by supplying household demand, vehicle-to-grid (V2G) operation by exchanging energy with the grid, and increased photovoltaic (PV) self-consumption by storing surplus solar generation. Unlocking this potential, however, requires control strategies that manage uncertainty in household demand and solar generation, satisfy user-driven mobility requirements, and avoid excessive battery wear.

This thesis develops an online framework for residential vehicle–home–grid energy management with rooftop PV integration. During each home-parking interval, energy flows among the EV battery, household load, grid, and PV system are scheduled using a shrinking-horizon model predictive control (SH-MPC) approach that updates decisions as new information becomes available. Battery lifetime effects are modeled by combining calendar and cycle aging mechanisms. To handle imperfect foresight, the controller is coupled with a neural-network-based forecaster to estimate future household load and PV generation. The control objective is to minimize total operating cost, jointly accounting for electricity purchase/sale and battery degradation expenses.

Simulation studies under Swedish residential conditions demonstrate that degradation-aware bidirectional charging can provide tangible economic value while maintaining acceptable battery aging. Sensitivity analyses confirm that these benefits persist across a wide range of operating scenarios and uncertainty levels.

Keywords: Electric vehicles, bidirectional charging, vehicle-to-grid, vehicle-to-home, battery aging, photovoltaic, model predictive control.

To everyone who supported me along the way.

List of Publications

This thesis is based on the following publications:

[A] **Francesco Popolizio**, Torsten Wik, Chih Feng Lee and Changfu Zou, "Online Aging-aware Energy Optimization for Vehicle-Home-Grid Integration". Submitted to *International Federation of Automatic Control (IFAC) World Congress*, Busan, Republic of Korea, Aug. 2026.

[B] **Francesco Popolizio**, Albert Škegro, Torsten Wik, Chih Feng Lee and Changfu Zou, "Online Energy Management for Bidirectional EV Charging with Rooftop PV: An Aging-Aware MPC Approach". Submitted to *IEEE Transactions on Transportation Electrification.*

Other publications by the author, not included in this thesis, are:

[C] **Francesco Popolizio**, Martina Vinetti, Alvin Combrink, Sabino Francesco Roselli, Maria Pia Fanti and Martin Fabian, "Online Conflict-Free Scheduling of Fleets of Autonomous Mobile Robots". *IEEE 20th International Conference on Automation Science and Engineering (CASE)*, Bari, Italy, Aug. 2024.

[D] Maria Pia Fanti, Agostino Marcello Mangini, Daniele Martino, Ignazio Olivieri, Fabio Parisi and **Francesco Popolizio**, "Safety and Comfort in Autonomous Braking System with Deep Reinforcement Learning". *IEEE International Conference on Systems, Man, and Cybernetics (SMC)*, Prague, Czech Republic, Oct. 2022.

Contents

Acknowledgments

I would like to express my sincere gratitude to my supervisors for their guidance, advice, and continuous support. In particular, I would like to thank my main supervisor, Changfu Zou, for his trust, his ambition, and for his steady guidance throughout this work. I have learned an enormous amount from him, not only from his technical insight but also from the dedication he brings to research every day. I am sincerely thankful to Torsten Wik and Chih Feng Lee for their supervision, insightful feedback, and continued encouragement, all of which have significantly shaped the direction and quality of my research. In addition, I would like to thank Albert Škegro for his support and for the collaboration over the last few months. His practical help and constructive discussions have been particularly valuable during the development and finalization of the journal article.

I also wish to thank my family and my friends for their encouragement and constant presence throughout this journey. Your support made the demanding moments easier and the good ones even more meaningful. A special thank you to Martina, who understands me like no one else. Thank you for believing in me and for being part of this path.

Acronyms

EV:	Electric Vehicle
PV:	Photovoltaics
V2X:	Vehicle-to-Everything
V2G:	Vehicle-to-Grid
V2H:	Vehicle-to-Home
G2V:	Grid-to-Vehicle
G2H:	Grid-to-Home
PV2V:	PV-to-Vehicle
PV2G:	PV-to-Grid
PV2H:	PV-to-Home
MPC:	Model Predictive Control
SH-MPC:	Shrinking-Horizon Model Predictive Control
SoC:	State-of-Charge
SoE:	State-of-Energy
SoH:	State-of-Health
LFP:	Lithium Iron Phosphate
NMC:	Lithium Nickel Manganese Cobalt Oxides
NN:	Neural Network
LSTM:	Long Short-term Memory

Part I

Overview

CHAPTER 1

Introduction

The electrification of mobility is accelerating worldwide, and electric vehicles (EVs) are rapidly becoming a significant share of residential electricity demand. EV sales exceeded 17 million globally in 2024, corresponding to a sales share above 20% [1]. In its 2025 outlook, the International Energy Agency (IEA) projected that 2025 EV sales would surpass 20 million (i.e., more than one-quarter of global car sales) [2]. This projection is consistent with subsequently released full-year market data reported in early 2026, which estimates global EV sales in 2025 at about 20.7 million units [3].

This sustained uptake is consistent with the Paris Agreement's long-term decarbonization goals, which call for deep emission cuts over time and imply a progressive transition away from fossil-fuel-based transport [4]. However, transport electrification implies a structural shift of final energy demand from liquid fuels to electricity. Transport accounts for about 30% of global final energy demand [5] and, as EV uptake scales, contributes to rising power consumption: global electricity demand grew by 4.3% in 2024 (vs. 2.5% in 2023) and is projected to remain around 3.9% over 2025–2027 [6].

The electricity demand growth is occurring in parallel with a structural transformation of supply, driven by the large-scale deployment of variable renewables, especially solar photovoltaics (PV). PV is one of the fastest-growing renewable energy sources, offering substantial benefits in terms of reducing greenhouse gas emissions and fostering energy independence. By 2030, renewables are projected to supply about 43% of global electricity generation (up from 32% in 2024), while renewable electricity generation is expected to reach about 16,200 TWh globally (up from about 9,900 TWh in 2024) [7]. At the household level, rooftop PV installations not only reduce emissions but also allow owners to decrease electricity costs by directly consuming their own solar generation, thereby increasing self-sufficiency. Moreover, surplus production can be injected into the grid, enabling owners to generate an additional source of income [8].

Despite these positive trends, high PV penetration increases the variability and uncertainty of net demand at the distribution level, due to weather-driven generation. Together with the rapid growth of electrified loads (including EV charging), this variability creates new operational challenges for power systems. A promising way to address these challenges is to utilize EV batteries enabled by bidirectional charging technologies, allowing EVs to function not only as loads but also as distributed energy storage resources.

The primary goal of traditional EV charging systems is to charge the battery once an EV is connected to the power socket [9]. However, a vehicle is parked approximately 96% of the time during a day, and this dwell time is much longer than the time needed to fully charge an EV battery [10]. This substantial idle time represents an opportunity for EVs to act as active participants in the power system, enhancing flexibility and facilitating the integration of renewable energy sources.

Bidirectional charging enables this idle time to be exploited in a value-creating manner for both the EV owner and the power system. Specifically, through vehicle-to-grid (V2G) and vehicle-to-home (V2H) operation, the energy stored in the EV battery can be exported to the grid or used to supply the household, respectively. In this sense, bidirectional charging transforms the EV from a passive load into a flexible, distributed energy node that can interact with the surrounding energy system when the EV is parked. This capability provides a natural interface to couple user-centric objectives (e.g., cost reduction) with system-level needs (e.g., flexibility under renewable variability) without compromising the vehicle's primary mobility function.

However, large-scale adoption of V2G and V2H requires more than technical feasibility: it ultimately depends on whether EV users perceive participation as economically attractive under realistic constraints (mobility needs, uncertain availability, and imperfect forecasts).

From the user perspective, bidirectional charging is appealing only if its benefits are tangible and easy to understand; in fact, user acceptance is widely recognized as a central bottleneck for large-scale deployment. Reported surveys and stated-preference studies indicate that clear financial value is a primary driver of interest, whereas concerns about reduced day-to-day flexibility, range anxiety, and potential battery wear often limit engagement [11–13]. In this context, V2H-oriented use cases are frequently perceived as more intuitive, since they translate directly into household benefits and may also provide added value during power interruptions [14, 15]. Moreover, rooftop PV is often viewed as a natural complement to bidirectional charging: surplus solar generation can be stored locally in the EV battery and later used within the household, increasing self-consumption and improving the overall value proposition of V2G/V2H operation [16–18].

These considerations motivate the need for control and market participation strategies that make the user-side economic case for bidirectional operation robust under realistic mobility and uncertainty constraints.

For this reason, the work presented in this thesis focuses on a user-centric value proposition for V2G based on energy arbitrage [19]—i.e., charging when electricity prices are low and discharging when they are high—and on V2H operation to increase household self-consumption (e.g., by using the EV to supply domestic demand). These services are assessed while explicitly accounting for two practical factors that determine user acceptance: range anxiety and EV battery degradation. Moreover, since an EV is not continuously available for grid interaction, the proposed approach is evaluated in an online setting that reflects time-varying vehicle availability and forecast imperfections.

From the user perspective, preserving mobility is paramount. Range anxiety reflects the concern that bidirectional operation may leave insufficient energy for the next trip; accordingly, empirical studies identify range requirements and perceived loss of flexibility among the main factors shaping willingness to participate in V2G/V2H programs [20, 21]. To mitigate range anxiety, a range of mobility-protection mechanisms can be adopted. These include embedding user-centric service-quality terms that penalize low state-of-charge (SoC) as a function of both the achieved SoC and the elapsed charging time [22, 23], enforcing explicit time-based SoC requirements (e.g., reaching and maintaining a minimum SoC after plug-in) [24], and gating bidirectional operation such that energy export is enabled only after the battery has reached a defined target SoC [25, 26].

A further key barrier to intensive bidirectional operation is battery degradation. While frequent cycling can improve the economic attractiveness of V2G/V2H (e.g., by increasing arbitrage opportunities), it can also accelerate aging [27], introducing an implicit cost for the EV owner and potentially offsetting the expected gains. Consequently, degradation-aware modeling is essential to obtain a realistic user-side cost–benefit assessment and to avoid operating strategies that appear profitable only under overly optimistic aging assumptions [28, 29].

Beyond mobility-related concerns and battery aging, bidirectional charging must also cope with real-time variability and uncertainty. In real-world operation, key inputs evolve over time—for instance household demand and PV generation—so approaches that assume perfect knowledge of future conditions can be overly restrictive. Instead, an online, rolling-horizon control strategy—often referred to as Model Predictive Control (MPC) [30]—is adopted, where decisions are regularly updated as new measurements and forecasts become available, naturally capturing time-varying conditions and forecast errors [31].

In summary, enabling bidirectional charging at scale requires control strategies that remain economically convincing for users while respecting mobility needs, battery aging, and time-varying operating conditions. It is therefore important to understand how EVs can be effectively integrated as flexible energy assets—through V2G and V2H operation, and potentially in coordination with rooftop PV—to enhance the value of bidirectional charging in practical settings. The next section formulates the research questions that guide this thesis.

1.1 Research Questions

The previous section motivates the need for user-centric and realistic approaches to bidirectional charging: the value of V2G and V2H must remain economically attractive while respecting user needs, battery aging, and time-varying operating conditions. To clarify the scope of this thesis and structure the remainder of the work, the following research questions are posed:

- *RQ1:* How economically beneficial is bidirectional charging (V2G/V2H) for an EV owner under realistic mobility constraints and battery degradation, and how does it compare to conventional unidirectional smart charging[1]?

- *RQ2:* To what extent does explicitly modeling battery degradation change the profitability and optimal charging/discharging decisions of bidirectional operation, compared with formulations that neglect degradation?

- *RQ3:* How can an online, degradation-aware MPC framework for vehicle-home-grid systems be formulated in the presence of incomplete information at decision time, while remaining feasible and economically effective under forecast errors?

- *RQ4:* What is the added value of rooftop PV within the proposed framework, and which key parameters (e.g., battery size, PV capacity, driving patterns) most strongly influence the overall cost–benefit balance?

1.2 Thesis Contribution

This thesis investigates user-centric bidirectional charging for a single EV owner in a Vehicle–Home–Grid framework, with a focus on economic value creation through V2G energy arbitrage and V2H household supply. The contributions of the thesis, including those presented in Papers A and B, are summarized as follows.

User-centric optimization framework. A modeling and optimization framework is developed to coordinate household electricity flows among the EV battery, the home, rooftop PV (when available), and the grid, with the objective of improving the user-side economic outcome while respecting practical requirements.

[1] Refereed to home charging, unidirectional smart charging lets the user set a departure time and a target charge level, while the system automatically schedules charging to take advantage of lower electricity prices (e.g., off-peak hours) and still meet the target by departure [32].

Degradation-aware bidirectional charging. The framework explicitly accounts for battery aging costs in the decision-making process, enabling a realistic assessment of the trade-off between potential arbitrage gains and the implicit cost of additional battery usage. In particular, semi-empirical degradation models are considered, capturing both calendar aging and cycle aging effects. The impact of including degradation modeling (versus neglecting it) is quantified in numerical studies.

Mobility-aware operation and range protection. The proposed control framework explicitly accounts for time-varying vehicle availability, and integrates mobility-related requirements into the decision-making process. In addition, user-centric constraints with service-quality formulations linked to the achieved state-of-charge are enforced to guarantee the desired energy level for upcoming trips. These constraints ensure that bidirectional operation does not compromise the vehicle's primary transport function.

Online (rolling-horizon) control under imperfect information. An online MPC-based strategy is adopted to handle time-varying and uncertain conditions (e.g., unknown future data, as well as forecast errors). When future inputs are not known at decision time, they are estimated using a neural-network-based forecasting model and updated at each receding-horizon step. Decisions are then re-optimized as new measurements and forecasts become available, enabling practical implementability compared to idealized, perfect-foresight optimization.

Benchmarking against unidirectional smart charging. The user-side value of bidirectional charging is evaluated by comparison to conventional unidirectional smart charging baselines, highlighting under which conditions bidirectional operation provides additional benefit.

Assessment of PV integration and sensitivity analysis. The added value of rooftop PV within the proposed framework is analyzed, together with key sensitivities and trade-offs (e.g., battery capacity, PV size, driving patterns, and price spreads), to characterize when and why the proposed approach is most effective.

1.3 Thesis Outline

The remainder of this thesis is organised as follows. *Chapter 2* introduces bidirectional charging concepts and the broader Vehicle-to-Everything (V2X) paradigm, of which Vehicle-to-Grid (V2G) and Vehicle-to-Home (V2H) are key operating modes. *Chapter 3* presents the battery degradation modeling, first introducing battery operation and the mechanisms driving degradation, and then focusing on the adopted semi-empirical models, which capture both calendar and cycle aging. *Chapter 4* describes the photovoltaic (PV) component, including basic modeling assumptions and the solar irradiance data used in the simulations. *Chapter 5* outlines the neural-network-based forecasting module, summarizing the considered model structures and the selected input features. *Chapter 6* formulates the Vehicle–Home–Grid–PV control problem and presents the proposed MPC-based coordination strategy, including the shrinking-horizon online implementation. *Chapter 7* summarizes the included papers (Paper A and Paper B) and clarifies their relation to the overall thesis narrative. Finally, *Chapter 8* concludes the thesis and discusses directions for future work.

CHAPTER 2

Bidirectional Charging

The electrification of road transport tightly couples two infrastructures that have traditionally been planned and operated largely independently: the mobility system and the electric power system. On the one hand, widespread adoption of EVs can reduce emissions and increase end-use energy efficiency; on the other hand, large-scale EV charging introduces new electrical loads, which may exacerbate peak demand, stress distribution assets, and affect local voltage profiles if left unmanaged. Comprehensive reviews of EV-grid integration emphasize that the magnitude of these impacts depends on EV penetration levels, charging power, temporal charging patterns, and the degree of coordination (or lack thereof) across users and network areas [33–35].

A key paradigm for mitigating adverse grid impacts while extracting additional value from electrified mobility is the smart grid. In essence, the smart grid extends the traditional power system with sensing, communication, and control, enabling more informed operational decisions across generation, networks, and end-users. This digitalization supports functionalities such as active management of distributed energy resources and coordinated demand-side flexibility, with the goal of improving efficiency, reliability, and the ability to integrate variable renewables [36, 37].

Within this paradigm, EVs can be treated not only as energy consumers but also as flexibility providers, because their charging process can be controllable in time and magnitude, and their batteries represent a distributed storage potential. Depending on the extent to which this flexibility is enabled at the charging interface, EV integration can be broadly organized into two fundamental operating paradigms, depending on the charging flow: unidirectional charging or bidirectional charging.

Unidirectional charging represents the standard case, in which power flows only from the electricity grid to the EV. In its simplest (uncontrolled) form, the EV starts charging as soon as it is plugged in. More advanced smart charging (or controlled charging) strategies instead schedule the charging power over time, for instance, to exploit time-varying electricity prices and charge when electricity is cheaper [38, 39], or to manage local power constraints by limiting peaks and sharing available capacity at charging sites [40]. In addition, smart charging can explicitly incorporate battery aging considerations to avoid overly aggressive operation and reduce degradation [41, 42].

Bidirectional charging extends the standard charging mode by enabling power to also flow from the EV battery back to external loads or the grid [33, 43].

Bidirectional charging is therefore the key technological enabler for a class of vehicle-to-everything applications, denoted as *Vehicle-to-X* (V2X).

The next subsection introduces the V2X paradigm, outlines the main operating modes (such as V2G and V2H), and discusses the key challenges associated with bidirectional charging strategies.

2.1 Vehicle-to-Everything (V2X)

Vehicle-to-Everything (V2X) builds on the idea that an EV can play a dual role. It is primarily a means of transportation, but when parked and connected, it can also act as an energy resource. Leveraging bidirectional charging, this flexibility can be accessed by managing charging and discharging power at the EV–charger interface, thereby allowing the EV to provide services beyond mobility. In the literature, V2X is used as an umbrella term covering multiple possible recipients of energy and/or flexibility—including the power grid, a home or building, dedicated local loads, or other vehicles—and thus encompasses a range of operational objectives and technical realiza-

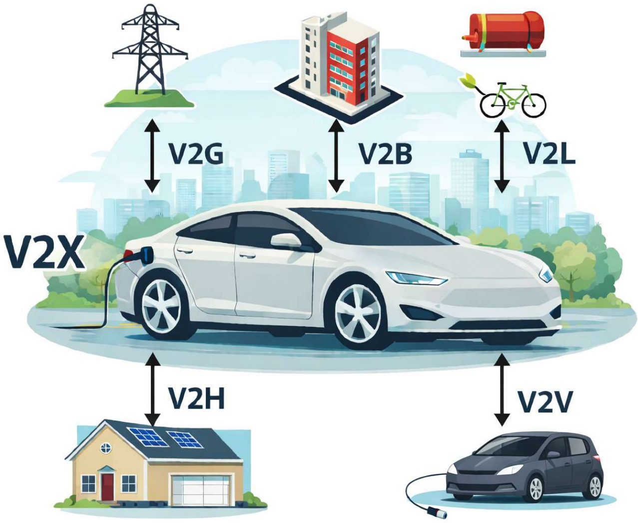

Figure 2.1: Illustration of the Vehicle-to-Everything (V2X) concept, showing an EV as a flexible energy asset capable of interacting with the power grid (V2G), buildings (V2B), external loads (V2L), homes (V2H), and other EVs (V2V) through bidirectional charging.

tions [44]. The growing interest in V2X is linked to the transition toward power systems with higher shares of variable renewable generation and increasingly electrified end-uses, where flexibility—the ability to shift or modulate electricity consumption and, when possible, to supply electricity back—is valuable across multiple time scales [43]. Importantly, the feasibility of each V2X mode is shaped by a combination of technical constraints (e.g., power ratings and efficiency), market and regulatory conditions (e.g., interconnection and remuneration rules), and user-centric requirements (e.g., availability windows and minimum state-of-charge to preserve mobility) [45].

The following subsections introduce the most common V2X modes—including Vehicle-to-Grid (V2G), Vehicle-to-Home (V2H), Vehicle-to-Building (V2B), Vehicle-to-Load (V2L), and Vehicle-to-Vehicle (V2V)—and refer to Fig. 2.1 for a compact visualization, highlighting their typical use-cases, key enabling assumptions, and main technical and regulatory considerations.

Vehicle-to-Grid (V2G)

Vehicle-to-Grid (V2G) denotes the operating mode in which an EV can exchange power bidirectionally with the electric grid while connected through a charger/charging station, so that the vehicle battery can be used as a controllable flexibility and storage resource at the grid interface [46, 47]. In contrast to unidirectional smart charging, where flexibility is provided only by shaping the charging demand, V2G enables both demand-side modulation and controlled power injection from the battery, thereby expanding the set of grid-oriented services that can be delivered [48].

Actors and operational structure. A typical V2G setup involves the EV (battery and onboard control), a bidirectional charger, and a coordination layer that may range from a local controller to an aggregator coordinating large EV fleets. Because individual EV availability is intermittent and user-driven, aggregation is highlighted as the practical pathway to provide higher capacity in grid services [43, 47]. Communication and interoperability between EV and chargers are therefore central to V2G implementation, and are increasingly framed around standardized interfaces (e.g., ISO 15118) [49].

Service categories

V2G can enable multiple services that may create economic value for the EV owner (or aggregator) and provide flexibility benefits to the power system. Among the most representative services discussed in the literature are energy arbitrage, peak reduction, and frequency regulation [48].

Energy arbitrage. Energy arbitrage relies on the fact that electricity prices are time-varying and that charging decisions can be shifted in time accordingly. In practice, this service is most naturally associated with home (or workplace) charging under dynamic or time-differentiated retail tariffs, where the end-user price is more directly linked to wholesale market conditions. By contrast, public charging is typically billed according to pricing schemes set by the charge point operator and/or the e-mobility service provider, which does not necessarily track short-term wholesale price variations [50, 51]. Under this premise, an EV can charge when electricity is inexpensive and discharge when prices are higher, effectively shifting energy in time. This can reduce net energy costs—or even generate profits—and contribute to a smoother net load, provided that bidirectional export is technically allowed and adequately remunerated [48].

Peak shaving. Electricity demand is not constant over the day and typically exhibits peaks driven by aggregated residential peaks and industrial and commercial activity. Such peaks increase the stress on generation and network assets and can lead to higher operating costs. V2G can contribute to peak reduction by coordinating charging away from peak hours and, when bidirectional export is available and economically justified, by discharging from EV batteries during peak periods, effectively injecting power to offset part of the demand and flatten the net load profile. Large-scale assessments indicate that V2G-enabled EVs can provide substantial peak-shaving potential under realistic mobility patterns and operational constraints [52].

Frequency regulation. Frequency regulation exploits V2G to help maintain the instantaneous balance between power supply and demand, since any mismatch is directly reflected in the system frequency. In interconnected power systems, the nominal frequency is typically 50 Hz in Continental Europe and 60 Hz in North America, and regulation actions aim to keep frequency deviations within acceptable limits around these nominal values [53, 54]. Frequency regulation is a service in which a balancing authority dispatches a regulation signal requesting adjustments of power. V2G-capable EVs can track such signals by modulating charging/discharging power around a baseline setpoint, and, since this regulation is a power service with limited net energy exchange over short time horizons, EV batteries can provide high-quality response while respecting state-of-charge and mobility constraints, provided that coordination and compensation mechanisms are in place [55].

Beyond these, the literature also discusses additional grid-support functionalities. For instance, V2G-capable chargers may provide voltage-support to avoid low voltage in the distribution network [56]; V2G control can support congestion management in distribution grids by coordinating EV charging and discharging to prevent line overloads in specific areas and time periods [57]; and, under specific technical and operational conditions, fleets of EVs have been investigated as potential contributors to black-start[1] and system

[1] A black-start is the process of restoring an electric power station, a part of an electric

restoration processes following wide-area outages [59].

Vehicle-to-Home (V2H)

Vehicle-to-Home (V2H) refers to the operating mode in which an EV can supply power to a residential load while connected at a household charging point, allowing the EV battery to act as a flexible home energy resource in addition to its mobility function [60]. In contrast to V2G, which targets grid-level objectives and market-based services, V2H is typically framed as an application where control decisions are driven by household energy management goals and local constraints [61].

Typical objectives and operating principle

The V2H literature most commonly motivates this mode through

- electricity cost reduction under time-varying tariffs (charging the EV battery from the grid when the prices are low and supplying part of the load from the EV through V2H when prices are high) [62],
- improved utilization of on-site generation such as PV by increasing self-consumption [63], and
- peak load reduction at the household level [64].

These goals are often formulated within a home energy management system that schedules EV charging/discharging together with domestic loads and local generation, subject to comfort and appliance constraints [63].

A distinctive value proposition of V2H is the backup supply during grid outages, where the EV can support critical household circuits or, depending on the installation, larger portions of the home load [65, 66].

Vehicle-to-Building (V2B) and Vehicle-to-Load (V2L)

Vehicle-to-Building (V2B) extends the V2H concept to a larger and often more controllable electrical demand, where an EV (or a fleet of EVs) can exchange power with a commercial or public building through bidirectional charging

grid or an industrial plant, to operation without relying on the external electric power transmission network to recover from a total or partial shutdown [58].

infrastructure and a building energy management system. From a functional perspective, V2B leverages the EV battery as a flexible resource to shape the building's net load profile, with typical objectives including peak demand reduction (notably relevant when demand charges apply) [67], cost reduction under time-varying tariffs, and improved utilization of on-site generation such as PV [68]. Compared to residential use, buildings can offer higher power levels and more predictable load patterns, which can simplify scheduling and increase the value of coordinated charging/discharging, while still requiring mobility-aware constraints for the participating vehicles.

Vehicle-to-Load (V2L), by contrast, refers to supplying local loads directly from the EV, typically through an outlet or a dedicated interface, without the need for providing services to the grid. V2L is therefore often framed as an application that emphasizes practicality and resilience: it can power appliances, tools, or temporary loads in locations where grid access is limited, and it can supply selected critical loads during outages [69].

Vehicle-to-Vehicle (V2V)

Vehicle-to-Vehicle (V2V) refers to the direct transfer of electricity between two EVs, where one vehicle temporarily acts as an energy source to charge another. The mode is typically motivated as a peer-to-peer support functionality, e.g., energy sharing, logistical operations (e.g., fleet support), or to enable emergency charging when fixed infrastructure is unavailable [60].

From an implementation perspective, V2V can be realized through (i) grid-mediated transfer (one EV discharges to the grid while another charges) or (ii) direct transfer using wired or wireless configurations that leverage existing onboard conversion stages (e.g., using the onboard charger interfaces) [70].

2.2 Key Challenges for Bidirectional Charging

Despite its potential, the deployment of bidirectional charging faces several challenges that span technology, operations, markets, and user acceptance.

Availability and uncertainty. EV availability is intermittent: the resource is only available when vehicles are plugged in, and connection/usage patterns are user-driven and uncertain. This creates variability in the capacity that can be committed to services and motivates forecasting, control, and aggregation strategies that can tolerate stochastic arrivals/departures [45].

Battery aging and incentives. Bidirectional charging increases the EV battery throughput and may accelerate degradation, introducing a fundamental trade-off between service value and battery degradation costs. Techno-economic analyses emphasize that EV participation requires incentive and compensation mechanisms that account for battery degradation, not only electricity prices, and that control strategies should be degradation-aware when cycling is frequent [71].

Mobility preservation and range anxiety. Since the primary function of an EV is transportation, bidirectional strategies must preserve mobility needs (e.g., minimum state-of-charge at departure) and avoid undermining user confidence. Behavioral barriers such as range anxiety and perceived inconvenience are identified as important determinants of acceptance and participation, reinforcing the need for user-centric constraints and incentive design [43].

Additional practical barriers to large-scale bidirectional charging deployment are beyond the scope of this thesis. *Interoperability and certification* remain critical, since real-world roll-out requires implementation of communication standards (e.g., ISO 15118-20 for EV–charger interoperability) and compliance with grid interconnection and protection requirements [49]. *Security and privacy* are also first-order concerns, as V2X expands the cyber-physical attack surface across vehicles, chargers, aggregators, and infrastructures, calling for privacy-preserving architectures [72]. Finally, *market design and value allocation* determine *who pays whom* (and for what) across EV owners, aggregators, charge point operators, and system operators: remuneration depends on service definitions as well as metering and settlement rules for bidirectional energy flows [43].

CHAPTER 3

Battery Degradation Modeling

In recent years, batteries have become a cornerstone of electrified transportation, enabling the large-scale deployment of EVs. Today, lithium-ion (Li-ion) technology dominates EV energy storage thanks to its favorable combination of high energy density, power capability, high round-trip efficiency, and technological maturity [73]. However, as EV penetration increases and batteries are increasingly used beyond pure mobility (e.g., fast charging and bidirectional operation), battery aging becomes a central technical and economic concern: capacity loss and resistance growth progressively reduce usable energy and power, affect vehicle range, and ultimately determine replacement needs and life-cycle cost.

This chapter provides the background and modeling tools needed to incorporate battery aging in energy management and control-oriented studies. It first reviews battery operating principles and the main notions required to interpret degradation phenomena. It then introduces the main battery degradation mechanisms and focuses on semi-empirical aging models, which are widely used in control applications to represent calendar aging and cycle aging through nonlinear stress-factor formulations. Next, the chapter surveys alternative modeling approaches, such as physics-based and data-driven modeling, and discusses their key advantages and limitations relative to semi-empirical models in terms of interpretability, data requirements, and suitability for optimization and controller design.

3.1 Battery Operating Principles

Lithium-ion batteries store and deliver energy through the reversible transport of lithium ions between two host materials: a negative electrode (anode) and a positive electrode (cathode), separated by a separator and soaked in a liquid electrolyte, as illustrated in Fig. 3.1. The separator prevents internal short-circuits between electrodes while allowing ionic conduction, whereas the electrolyte (typically a lithium salt dissolved in organic carbonate solvents) provides the medium for Li-ion transport within the cell [74].

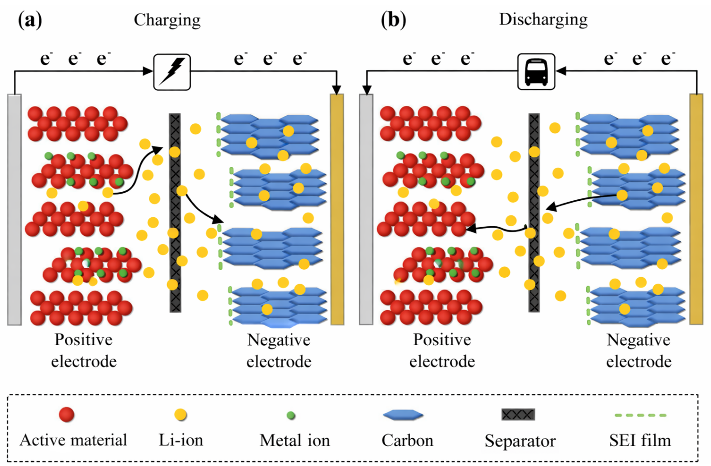

Figure 3.1: Charging and discharging principles of Li-ion batteries [74].

During discharge, Li-ions move from the negative electrode to the positive electrode through the electrolyte and the separator, while electrons flow through the external circuit to power the connected load. During charge, an external power source reverses these flows: Li-ions travel from the positive electrode back to the negative electrode inside the cell, and electrons are driven in the opposite direction through the external circuit [75].

From a materials perspective, the negative electrode in commercial EV cells is most commonly graphite, sometimes blended with silicon to increase capacity, whereas the positive electrode is typically composed of metal oxides, such as nickel-manganese-cobalt (NMC), or lithium-iron-phosphate (LFP) [76]. A key interfacial feature is the solid electrolyte interphase (SEI), which forms mainly on the negative electrode surface during the initial cycles due to electrolyte reduction [77].

From Cell to Battery Pack

Battery operation and degradation are often described at the cell level. In practice, however, an EV battery refers to a pack composed of many cells connected in series and parallel, typically organized into modules [74]. Series connections increase the operating voltage, while parallel connections increase the usable capacity and allowable current. To a first approximation,

$$V_{\text{pack}} \approx N_s \, V_{\text{cell}}, \qquad Q_{\text{pack}} \approx N_p \, Q_{\text{cell}}, \tag{3.1}$$

where N_s and N_p denote the number of cells in series and in parallel, respectively, V denotes voltage, and Q denotes (charge) capacity (ampere-hour, Ah).

Regarding typical voltage levels, the nominal cell voltage depends on the chemistry (e.g., around 3.2 V for LFP cells [74], and around 3.6–3.8 V for NMC-based cells [78]). At the pack level, mainstream EV platforms have historically adopted ∼400 V architectures, while ∼800 V systems are increasingly used to enable high-power fast charging with lower current levels [79].

3.2 Battery Degradation

Lithium-ion batteries do not maintain their initial performance indefinitely: as time passes and the cell is used, the available capacity and power capability gradually decrease, while internal resistance typically increases. This aging process is the result of several coupled physical and electrochemical mechanisms taking place inside the cell, whose impact depends strongly on operating conditions such as temperature, SoC, charge/discharge rate, and depth of cycling.

From a high-level perspective, two mechanisms are often highlighted as particularly relevant in automotive Li-ion cells. First, the SEI forms mainly on the negative electrode during the initial cycles due to electrolyte reduction. While the SEI is beneficial because it passivates the anode surface and helps stabilize the electrode–electrolyte interface, its gradual growth over time can consume cyclable lithium and increase impedance, contributing to capacity fade and power loss [77, 80]. Second, under unfavorable charging conditions—most notably low temperatures, high charging currents, or high SoC—lithium plating may occur, meaning that metallic lithium is deposited on the anode surface instead of being inserted into the host material. This process reduces usable capacity, can accelerate further degradation, and in severe cases raises safety concerns [81].

Beyond SEI growth and lithium plating, additional aging phenomena may develop concurrently, including loss of active material due to particle cracking, structural changes in electrode materials, electrolyte degradation, and current-collector or contact degradation [77, 80]. Importantly, these mechanisms can reinforce each other, making battery degradation highly path-dependent.

3.3 Semi-Empirical Nonlinear Modeling

Battery models can be formulated at different levels of detail to represent electrical, thermal, electrochemical, and aging-related phenomena, depending on the intended application and time scale. This section focuses on semi-empirical nonlinear degradation models, adopted in both Paper A and Paper B, because they offer a practical compromise between physical interpretability, predictive accuracy within a calibrated operating region, and computational tractability for simulation- and control-oriented studies [77].

Rather than explicitly resolving internal electrochemical states and side-reaction dynamics, semi-empirical models describe aging through compact nonlinear relationships calibrated on laboratory data. In doing so, they relate the evolution of state-of-health (SoH) indicators to measurable operating conditions such as temperature, SoC, depth-of-discharge, current rate, and cumulative energy or charge throughput.

Health Indicators

Semi-empirical degradation models typically track one or two aggregated health indicators: (i) *capacity loss*, i.e., the gradual reduction of the maximum charge that can be stored and delivered, and (ii) *resistance growth*, i.e., the increase in internal resistance that reduces power capability and increases losses. These indicators are often represented as deviations from initial values, e.g.,

$$Q_{\text{loss}}(t) = Q_0 - Q(t), \qquad R_{\text{loss}}(t) = R(t) - R_0. \tag{3.2}$$

Although battery aging manifests in both capacity loss and internal resistance growth, it is common—especially in control- and range-oriented studies—to quantify degradation using capacity loss alone. This choice is mainly motivated by the fact that capacity loss directly translates into reduced usable energy (and thus driving range), which is often more critical than the typically more marginal power limitation induced by resistance rise [82–84]. This simplifying assumption is also adopted in Paper A and Paper B.

Decomposition into Calendar and Cycle Aging

A common and practical structure decomposes total degradation into a calendar contribution, associated with time-dependent side reactions occurring during storage or low activity, and a cycle contribution, associated with charge–discharge operation. For a generic degradation modeled as battery capacity loss, this is commonly written as

$$Q_{\text{loss}} \approx Q_{\text{loss}}^{\text{cal}} \; + \; Q_{\text{loss}}^{\text{cyc}}. \tag{3.3}$$

This split is a widely used assumption: calendar and cycling aging are typically identified separately and then combined via a superposition (additive) approximation, while any coupling effects are neglected [85].

Calendar Aging

Calendar aging captures degradation that occurs primarily as a function of time and storage conditions, even in the absence of significant cycling. In semi-empirical formulations, it is commonly expressed as a cumulative capacity loss term

$$Q_{\text{loss}}^{\text{cal}}(t) = k_{\text{cal}}(T, \text{SoC})\, t^{\alpha}, \tag{3.4}$$

where t denotes elapsed time and $k_{\text{cal}}(\cdot)$ is a stress factor that collects the influence of the main stress factors, typically temperature T and storage SoC (or equivalently storage voltage). The exponent α is often chosen sublinear, with $\alpha = \frac{1}{2}$ being a widely used assumption, motivated by diffusion-limited growth processes (commonly associated with SEI evolution) that lead to an approximately square-root-of-time behavior [86, 87]. This behavior is illustrated in Fig. 3.2a, which highlights the time-driven accumulation of $Q_{\text{loss}}^{\text{cal}}$ under fixed storage conditions.

The temperature dependence of the stress factor k_{cal} is frequently modeled through an Arrhenius-type relationship:

$$k_{\text{cal}}(T, \text{SoC}) = k_{\text{cal,ref}}(\text{SoC}) \exp\left(-\frac{E_{a,\text{cal}}}{R}\left(\frac{1}{T} - \frac{1}{T_{\text{ref}}}\right)\right), \tag{3.5}$$

where $E_{a,\text{cal}}$ is an activation energy, R is the universal gas constant, and T_{ref} is a reference temperature. SoC effects are commonly included via an empirical dependence in $k_{\text{cal,ref}}(\cdot)$, reflecting that calendar aging rates can increase at higher storage SoC for many Li-ion chemistries [85, 88].

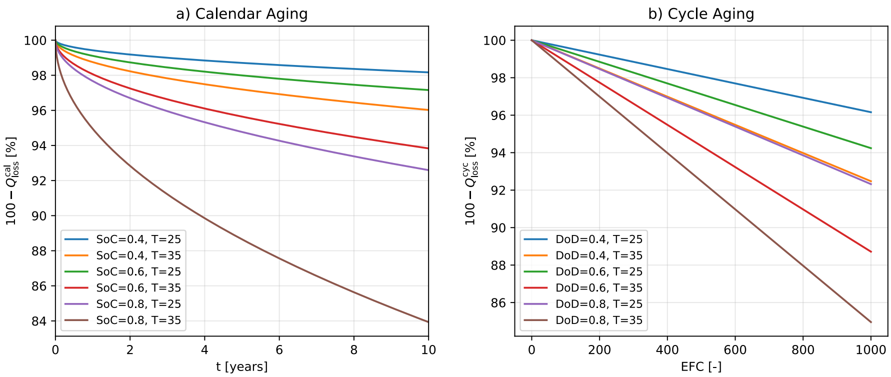

Figure 3.2: Calendar and cycle aging trends for NMC cells based on the semi-empirical model in [88]: (a) calendar aging under different storage SoC and temperature conditions; (b) cycle aging under different DoD and temperature conditions.

Cycle Aging

Cycle aging captures degradation driven by charge–discharge operation and is therefore primarily linked to cumulative usage. A common semi-empirical representation expresses the cycling-induced capacity loss as

$$Q_{\text{loss}}^{\text{cyc}} = k_{\text{cyc}}(T, \text{DoD}, C\text{-rate}, \dots)\ N_{\text{EFC}}^{\beta}, \tag{3.6}$$

where N_{EFC} denotes the number of equivalent full cycles (EFC), $\beta \in (0, 1]$, and $k_{\text{cyc}}(\cdot)$ captures the impact of the dominant cycling stress factors, most commonly temperature T, depth of discharge (DoD), and C-rate [77, 85]. Fig. 3.2b, illustrates the cycling-driven accumulation of $Q_{\text{loss}}^{\text{cyc}}$ as a function of throughput (expressed via EFC in (3.6)) under different cycling stress factors.

EFC provides a throughput-based measure of cycling exposure: it counts how many full charge–discharge cycles the battery has effectively experienced in terms of processed charge. DoD quantifies the amplitude of the SoC swing over a cycle (or over a selected interval), typically defined as $\text{DoD} = \text{SoC}_{\text{max}} - \text{SoC}_{\text{min}}$. The C-rate expresses how aggressive the current is relative to the nominal capacity (1C corresponds to a one-hour (dis)charge at the nominal battery capacity). Higher C-rates and larger DoD, especially at unfavorable temperatures, typically accelerate cycle aging [27].

The stress-factor term $k_{\text{cyc}}(\cdot)$ can be parameterized in different ways: temperature is often modeled via an Arrhenius-type exponential dependence, while DoD and C-rate effects are captured through empirical (e.g., polynomial, exponential, or hybrid) functions identified from cycling tests. Other functional forms have been proposed in the literature; however, the power-law dependence in (3.6) is widely used due to its simplicity and practical effectiveness [86].

Strengths and Limitations

Semi-empirical degradation models are attractive for system-level studies and control design because they are compact, require limited computational resources, and rely on input variables that are typically available in a battery management system. Moreover, the calendar–cycle decomposition provides a modular structure that aligns with common aging-test protocols and facilitates the accumulation of degradation along arbitrary operating profiles [86].

At the same time, their predictive reliability is tied to the calibration domain: extrapolation beyond the tested ranges of temperature, SoC, DoD, or C-rate may lead to significant errors. In addition, these models provide an aggregated description of degradation and do not explicitly represent internal states or the detailed interaction of aging mechanisms. Finally, despite their relative simplicity, semi-empirical formulations are often nonlinear, which can complicate their direct integration into real-time control and optimization frameworks and may require suitable reformulations or approximations for tractable and efficient problem solving.

State-of-Charge (SoC) vs. State-of-Energy (SoE)

In the battery modeling literature, semi-empirical aging models are often expressed as functions of the SoC, which represents the remaining charge normalized by the nominal capacity (typically expressed in Ah) [85]. In Paper A, we follow this convention and use the SoC notation. In Paper B—and in Chapter 6 of this thesis—we instead use the state-of-energy (SoE), which represents the remaining energy normalized by the nominal energy capacity (typically expressed in kWh), since the energy management problem is naturally formulated in energy units. Under the common assumption of an approximately constant open-circuit voltage over the operating range, SoC and SoE are numerically equivalent and can therefore be used interchangeably.

3.4 Alternative Modeling Approaches

While this thesis and both Paper A and Paper B adopt a semi-empirical degradation model due to its favorable balance between accuracy and computational tractability, other modeling paradigms are also common in the literature for lithium-ion batteries. In particular, physics-based models describe aging from electrochemical and mechanical principles, whereas data-driven approaches infer degradation behavior directly from data. The following sections briefly outline these alternatives and summarize their main conceptual differences relative to semi-empirical modeling.

Physics-based Nonlinear Modeling

Physics-based models represent cell dynamics and degradation mechanisms through governing equations derived from charge and mass conservation laws, coupled with constitutive relations describing interfacial reaction kinetics and multi-phase transport processes. In contrast to semi-empirical aging models that prescribe degradation laws through fitted functional relationships based on physically motivated stress factors (e.g., DoD, temperature, or equivalent full cycles), physics-based models enable the estimation of internal state variables, such as concentration and potential distributions, which are not directly measurable but fundamentally govern degradation evolution [89–91].

A common foundation of physics-based battery modeling is porous-electrode theory, leading to the pseudo-two-dimensional (P2D) or Doyle–Fuller–Newman (DFN) model family [92, 93], which is typically formulated as a set of coupled, nonlinear differential equations. Degradation can then be included by augmenting the electrochemical model with additional submodels (e.g., SEI growth or lithium plating) [94]. While this approach can improve interpretability and extrapolation capability, it comes at the cost of substantially increased model order and parameterization effort. In particular, physics-based models involve high-dimensional internal states, require detailed parameter identification, and often lead to numerically intensive simulations, which can limit their direct use in real-time control compared to compact semi-empirical formulations [90]. For control-oriented applications, reduced-order physics-based models, such as the single-particle model (SPM) and its extensions, are often considered to alleviate the computational burden while retaining key physics; however, they still require careful parameterization and may remain challenging to embed in real-time optimization and control [95].

Data-driven Modeling

Data-driven approaches model battery behavior and aging by learning relationships directly from measurement data, with limited reliance on explicit electrochemical assumptions. In the context of degradation, data-driven approaches typically learn mappings from measurable signals (e.g., current, voltage, temperature) and their extracted features to health indicators such as capacity fade, resistance growth, or state-of-health. Importantly, "data-driven" does not imply a nonlinear model: depending on the intended use and available data, one may employ linear regression or identified linear dynamical models, as well as nonlinear machine-learning (ML) models such as Gaussian processes, decision-tree ensembles, or neural networks [96, 97].

A key motivation for data-driven modeling is its flexibility: by not committing to a specific mechanistic structure, these models can capture complex interactions among stress factors and operating regimes that may be difficult to represent with parametric laws. Moreover, once trained, many data-driven models can be evaluated efficiently, which can be attractive for online monitoring and prediction. However, this flexibility comes with several challenges. First, predictive performance is strongly dependent on data quality and coverage: models may fail when operating conditions differ significantly from those seen during training, and extrapolation outside the training domain can be unreliable. Second, measurement noise, sensor bias, and dataset heterogeneity (different cell batches, chemistries, or usage patterns) can lead to poor generalization if not carefully addressed through preprocessing, regularization, and validation. Third, the resulting models may be difficult to interpret and may produce non-physical predictions unless additional constraints or physics-informed structures are imposed [97].

From a control and optimization standpoint, data-driven models introduce additional considerations. While linear data-driven models can often be embedded directly in optimization-based controllers, more complex nonlinear models may be harder to use within a real-time optimization. Moreover, causality can become a critical issue: some data-driven models are developed for prediction accuracy rather than online decision-making and may rely, explicitly or implicitly, on non-causal information (e.g., future measurements or offline preprocessing), which limits their direct applicability in real-time control and optimization.

Comparison and Key Trade-Offs

Semi-empirical aging models provide a compact and interpretable structure (e.g., an explicit calendar and cycle decomposition with predefined stress-factor dependencies), yielding transparent links between operating conditions and degradation and making them well-suited for control-oriented analyses within a calibrated operating region. Physics-based models, in contrast, describe aging from electrochemical and transport principles and can expose physical internal variables, but they typically involve higher model complexity and a more demanding parameterization and simulation effort. Data-driven approaches offer increased modeling flexibility by learning degradation behavior directly from data without assuming a specific functional form; however, their reliability depends on the representativeness of the training data and on safeguards to ensure physical consistency and robust extrapolation.

In summary, physics-based models offer the strongest mechanistic grounding but are often the most demanding in terms of complexity and computational burden; data-driven models can be highly flexible but depend strongly on data quality and validation; semi-empirical models strike a balance by capturing the dominant aging dependencies with a compact, interpretable formulation. In this thesis—and in Paper A and Paper B—semi-empirical degradation models are adopted as a control-oriented compromise that remains computationally tractable while capturing the key stress-factor effects relevant to battery aging.

CHAPTER 4

Photovoltaic System as Renewable Source

Photovoltaic (PV) generation has become one of the most widespread and accessible renewable technologies for household applications, thanks to its modularity, declining costs, and the possibility of directly supplying local electrical demand. In the context of residential energy systems, rooftop PV can partially offset grid imports, reduce exposure to time-varying electricity prices, and contribute to decarbonization by replacing energy otherwise drawn from fossil-based generation [7].

In this thesis—and Paper B—PV is considered as an additional energy resource interacting with the home, the EV, and the public grid. Its presence introduces a daily and seasonal renewable power profile that can be exploited to increase self-consumption, support EV charging needs, and, when possible, sell surplus energy back to the grid. At the same time, PV generation is intermittent and weather-dependent, which motivates a characterization of the solar resource and its typical patterns.

In the literature, residential PV installations are often complemented by a stationary battery energy storage system to increase PV self-consumption and mitigate the mismatch between midday generation and evening demand. However, when an EV is available at home for a significant fraction of the day, the EV battery can provide a large and already-installed storage capacity, potentially reducing (or even removing) the need for an additional stationary battery. Several studies report that integrating PV with V2H operation can substantially increase self-consumption and self-sufficiency, and that adding both an EV and a stationary BESS is often less cost-effective than leveraging the EV battery as the primary storage unit [98–100].

This chapter provides the background on photovoltaic generation from a system perspective. It first outlines the PV modeling and operational aspects within the considered vehicle-home-grid energy architecture and discusses the main characteristics of the solar resource (e.g., diurnal cycles and seasonal variability) that shape the available renewable power. Finally, it summarizes the key modeling assumptions and simplifications adopted in this thesis and Paper B, to represent PV generation in a control-oriented and simulation-ready form.

4.1 Modeling and Operation

PV generation converts incident solar irradiance into electrical energy through an array of semiconductor modules connected to an inverter. PV modules are typically characterized by a rated (peak) power under standard test conditions (STC), i.e., a cell temperature of 25°C and a solar irradiance of 1000 W/m^2 (= 1 kW/m^2). The corresponding rating, usually expressed in Wp or kWp, represents the maximum power that the module can deliver under these reference conditions [101].

In real operation, the electrical output depends on multiple factors, including irradiance level, module temperature, and installation characteristics such as tilt and orientation. While irradiance primarily determines the instantaneous available solar resource, deviations from the optimal inclination and increases in cell temperature typically reduce the conversion efficiency and thus the delivered power [102]. Since the focus of this thesis is on system-level energy management rather than PV component design, a simplified PV representation is adopted in Paper B to capture the dominant time variability of solar generation with limited modeling complexity.

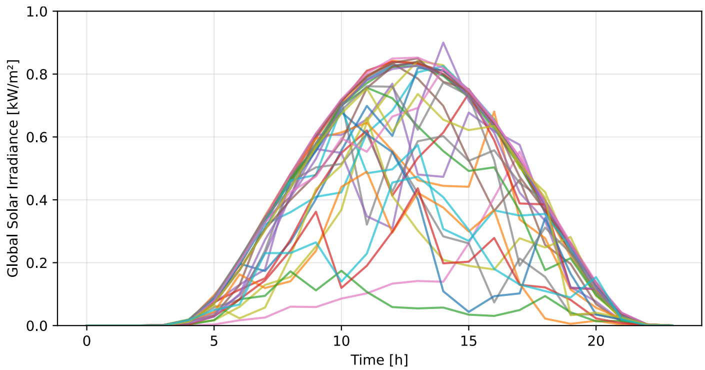

Figure 4.1: Global solar irradiance measured for 30 days in June 2020, showing the daily variability across the month for solar irradiance registered in Gothenburg, Sweden [103].

Equivalent Plant PV Model

PV generation is represented through an equivalent aggregate plant described by a nominal rating $P_{\text{nom}}^{\text{PV}}$ and a normalized solar irradiance profile $\text{SR}(t) \in [0, 1]$. The PV output at time step t is modeled as

$$P^{\text{PV}}(t) = \text{SR}(t)\, P_{\text{nom}}^{\text{PV}}, \qquad \text{SR}(t) \in [0, 1]. \tag{4.1}$$

The $\text{SR}(t)$ profile is obtained from the measured *global solar irradiance* $S(t)$ (in W/m^2 or kW/m^2) via a normalization with respect to the STC irradiance level,

$$\text{SR}(t) = \frac{S(t)}{S_{\text{ref}}}, \qquad S_{\text{ref}} = 1000\ \text{W/m}^2\ (= 1\ \text{kW/m}^2). \tag{4.2}$$

Under this abstraction, PV generation is zero during nighttime and follows the typical diurnal pattern, with peak values around solar noon and substantial day-to-day variability driven by weather and season.

To provide an empirical illustration of the solar resource, Fig. 4.1 reports the global solar irradiance $S(t)$ over a full month: the plot shows how irradiance evolves within the 24-hour cycle. The figure highlights the characteristic day–night pattern—with $S(t) \approx 0$ during nighttime hours and a pronounced peak around solar noon—as well as the day-to-day variability due to changing weather conditions.

Although the model above uses an aggregate rating $P^{\mathrm{PV}}_{\mathrm{nom}}$, it can be interpreted as the result of an array of N_{mod} modules, each rated at $P^{\mathrm{mod}}_{\mathrm{nom}}$ under STC, i.e.,

$$P^{\mathrm{PV}}_{\mathrm{nom}} = N_{\mathrm{mod}}\, P^{\mathrm{mod}}_{\mathrm{nom}}. \tag{4.3}$$

Modern residential modules typically occupy on the order of 1.7–2.0 m^2 per panel and have rated power in the range of $\sim$ 350–500 Wp [102, 104]. Consequently, at peak conditions (i.e., $\mathrm{SR}(t) \approx 1$) a single module can produce approximately 0.35–0.50 kWh over one hour.

Discrete-Time Energy Representation

The energy management problem is formulated with an hourly sampling time $\Delta t = 1$ h. Therefore, the PV energy produced over one time step can be written as

$$E^{\mathrm{PV}}(t) = P^{\mathrm{PV}}(t)\, \Delta t. \tag{4.4}$$

With $\Delta t = 1$ h, power in kW and energy per time step in kWh coincide numerically (though not dimensionally). For consistency with the time-discretized scheduling formulation used in the related papers, PV generation may thus be reported either as $P^{\mathrm{PV}}(t)$ [kW] or equivalently as $E^{\mathrm{PV}}(t)$ [kWh] over the hourly interval.

Practical Assumptions for PV Modeling

To keep the PV model aligned with the scope of this thesis and Paper B, detailed component-level effects are not explicitly modeled. In particular, a favorable tilt angle and a constant cell temperature of 25°C are assumed, so that the dominant dependency of PV output is captured through the irradiance-driven profile $\mathrm{SR}(t)$ derived from the global solar irradiance $S(t)$. This choice enables integrating PV generation into the vehicle–home–grid scheduling problem without introducing additional uncertain parameters (e.g., temperature dependence, shading, and orientation losses) that are not central to the control objective.

CHAPTER 5

Handling Uncertainty via Neural Network Forecasts

The vehicle–home–grid framework, extended with rooftop PV, is characterized by data that are only partially observable ahead of time. For instance, on the household side, enabling V2H operation requires knowledge of the household electricity demand, since this profile determines how much energy can be supplied by the EV (or must be drawn from the grid) at each time. Similarly, on the PV side, planning how PV energy should be allocated (for example, to serve household loads, charge the EV, or export to the grid) requires anticipating the PV generation.

These quantities are naturally available in real time, and their past values are known from measurements; however, their future trajectories over the next hours cannot be directly observed. This lack of foresight introduces a fundamental limitation when planning energy exchanges over a time horizon: without reliable estimates of future demand and/or PV production, decisions can only be made shortsightedly or based on overly conservative assumptions. One practical way to mitigate this issue is to predict these signals from historical data (and, when available, additional explanatory variables), thereby providing the controller with plausible future input profiles.

This chapter focuses on forecasting such uncertain inputs. Specifically, it addresses short-term prediction of unknown data over a finite horizon, using point forecasts produced by neural networks.

The chapter first defines the forecasting setup and describes the datasets used. It then presents the feature engineering and selection methodology, including permutation importance to assess the relevance of candidate inputs. Finally, it describes the neural-network models used for short-term forecasting, with emphasis on the architectures adopted in Paper A and Paper B.

5.1 Forecasting Setup and Data Description

This section formalizes the forecasting task considered in this thesis and summarizes how the datasets are constructed. The overall goal is to produce short-term predictions of uncertain input data at an hourly resolution, based on historical measurements available up to the current time.

One-Step-Ahead Forecasting Task

We consider a discrete-time setting with sampling time $\Delta t = 1$ h. At each time step k, the forecaster receives as input a look-back window covering the most recent 24 hours, i.e.,

$$\mathbf{x}(k) \triangleq \big[y(k-23),\, y(k-22),\, \ldots,\, y(k)\big], \tag{5.1}$$

which contains the 23 previous hourly measurements together with the current one. The forecasting model outputs a one-step-ahead point prediction,

$$\hat{y}(k+1|k), \tag{5.2}$$

representing the estimate of the next-hour value based on the information available at up to time k. Additional covariates that are known at time k may be appended to the input vector; their selection is discussed in Section 5.2.

Multi-Step Prediction via Recursive Forecasting

Although the model is trained for one-step-ahead prediction, forecasts over a longer horizon can be obtained through a recursive strategy. Starting from the one-step prediction $\hat{y}(k+1|k)$, the model is iteratively re-evaluated by

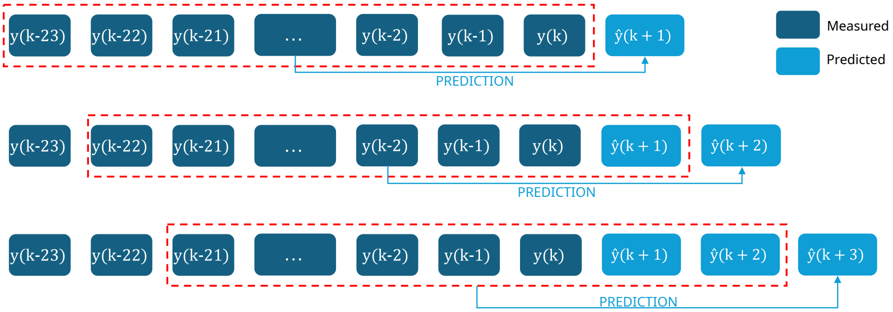

Figure 5.1: Recursive multi-step forecasting: starting from a 24-hour input window, the model predicts the next value, which is then fed back into the input to generate subsequent predictions (shown here for three steps ahead, i.e., $H = 3$).

augmenting the input window with the most recently predicted value, thereby generating

$$\hat{y}(k+2|k),\ \hat{y}(k+3|k),\ \ldots,\ \hat{y}(k+H|k) \tag{5.3}$$

over a finite horizon of H hours. An illustration of the recursive prediction procedure is shown in Fig. 5.1. This recursive procedure enables multi-step predictions without retraining separate models for each lead time, at the cost of a potential accumulation of prediction errors as the horizon increases [105].

Datasets Overview

Two datasets are considered in this thesis, reflecting the forecasting tasks addressed in the two companion papers. In Paper A, the forecasting model is trained using historical measurements of household electricity consumption. In Paper B, the forecasting setup is extended by considering both household consumption data and a solar-related time series (i.e., solar irradiance) to support short-term prediction in PV-integrated scenarios. The sampling time $\Delta t = 1$ h is also dictated by the temporal resolution of the adopted datasets.

Regarding household demand, a public dataset from the United States is used. From this dataset, five individual apartments located in the State of Washington were selected. This choice is motivated by the fact that Washington State exhibits climatic conditions that are broadly comparable to those of Northern Europe and Scandinavia, for instance southern Sweden.

Regarding PV-related data, a dataset containing solar irradiance measurements recorded in Gothenburg, Sweden, is used.

For further details on the two datasets, as well as on the preprocessing steps and the adopted training/validation/test split, the reader is referred to Paper A and Paper B, and to the dataset sources in [103, 106].

5.2 Feature Engineering and Selection

Forecasting performance strongly depends on how the available measurements are represented and which candidate inputs are provided to the model. This section discusses feature engineering and feature selection in the context of the considered forecasting problem. The focus is primarily on the feature set explored in Paper B, where a larger pool of candidate inputs was available (with partial overlap with the features used in Paper A). In such settings, a systematic selection step can be used to reduce the input dimensionality while retaining the most informative predictors. The following subsections introduce the candidate features and their representation, and then describe a selection methodology to identify a compact feature set.

Candidate Input Features

Building on the datasets introduced in Section 5.1, for the case study including both a household and PV, the two main time series extracted from the adopted sources are the household electricity consumption and the solar irradiance.

In addition to these primary variables, further candidate features can be constructed. Typical examples include time-related descriptors (e.g., hour of day or day of week) as well as additional variables available in [103].

In particular, for the case study selected—and considered during the preparation of Paper B—eight candidates can be selected as potential input features: household load, solar irradiance, humidity, temperature, wind speed, hour of the day, day of the week, and day of the year. Both humidity, temperature, and wind speed can be extracted from the dataset in [103].

Feature Importance

To determine which of these features are most informative for the prediction of the household load and the solar irradiation, a Permutation Feature Importance (PFI) analysis [107] is performed on the trained Transformer. PFI quantifies the relevance of a feature by measuring the degradation in prediction accuracy when its values are randomly permuted.

Setting

Let $X_{\text{test}} \in \mathbb{R}^{N \times L \times F}$ denote the test tensor (with N samples, window length L=24, and F features), and let the model produce two outputs: household load and solar irradiance. The baseline error, based on the mean squared error (MSE), is computed by

$$\text{MSE}^{\text{base}} = \underbrace{\text{MSE}\big(y_{\text{test}}^{\text{load}}, \hat{y}^{\text{load}}\big)}_{\text{load}} + \underbrace{\text{MSE}\big(y_{\text{test}}^{\text{solar}}, \hat{y}^{\text{solar}}\big)}_{\text{solar}},$$

i.e., the sum of the mean squared errors on both outputs.

Permutation step

For each feature index $i \in \{1, \ldots, F\}$, we create a perturbed copy $X_{\text{test}}^{(i)}$ by permuting all entries of the i-th feature across the entire test set and window, i.e., we flatten the $N \times L$ slice $X_{\text{test}}[:, :, i]$ to a vector, apply a random shuffle, and then reshape it back to $N \times L$. This destroys the temporal and cross-sample alignment of that feature while keeping its value distribution intact. We then recompute the model outputs and the corresponding error

$$\text{MSE}^{(i)} = \text{MSE}\Big(y_{\text{test}}^{\text{load}}, \hat{y}^{\text{load},(i)}\Big) + \text{MSE}\Big(y_{\text{test}}^{\text{solar}}, \hat{y}^{\text{solar},(i)}\Big).$$

The importance score for feature i is defined as the error increase:

$$I_i = \text{MSE}^{(i)} - \text{MSE}^{\text{base}}.$$

Higher I_i indicates greater relevance of feature i for the joint (two-output) forecasting task.

Iterative selection

Starting from the eight candidate features introduced above, an iterative pruning process is then applied to identify the most relevant subset using the computed PFI scores. The procedure is summarized in Algorithm 1.

Algorithm 1 Iterative feature selection using Permutation Feature Importance (PFI)

```
Initialize feature set F = {all candidate features}.
repeat
    Train the model using the current F.
    Evaluate baseline error MSE^base on the test set.
    Compute permutation importance I_i for all i ∈ F.
    Remove feature(s) with a low I_i value(s) from F.
until model accuracy does not improve or F reaches a desired size
Output: final selected feature set F*.
```

An iterative procedure similar to the one described above was applied during the preparation of Paper B, resulting in the following four features, which provided the best trade-off between forecasting accuracy and input dimensionality:

- household load
- solar irradiance
- day of the year (ranging from 1 to 365)
- hour of the day (ranging from 0 to 23)

Among the discarded features, day of the week was found to be redundant, as its periodic pattern is already encoded in the day of the year feature. Similarly, humidity, temperature, and wind speed exhibited low influence since their effects are implicitly captured by the measured solar irradiance, which already reflects the combined influence of these weather conditions on the available sunlight.

5.3 Neural Network Forecasting Models

This section provides an overview of neural network model families that are commonly used for short-term forecasting of time-series data. The aim is to outline the main modeling ideas and the typical input–output structure adopted in practice. After a brief introduction, recurrent models based on Long Short-Term Memory (LSTM) networks are discussed, including hybrid variants that combine sequence modeling with additional inputs. The section then introduces attention-based Transformer models, which have recently become popular for time-series forecasting. Finally, a short overview of other widely used alternatives is provided for completeness.

Overview: Neural Networks for Short-Term Forecasting

Machine learning refers to a class of methods that enable computers to learn patterns from data and improve performance on a task without being explicitly programmed with task-specific rules [108]. Within machine learning, artificial neural networks (NNs) denote a family of models built by composing multiple nonlinear transformations, whose parameters are learned from data [109].

Conceptually, artificial neural networks were originally inspired by simplified abstractions of biological neurons, with the aim of learning an input–output mapping directly from data [110]. In its basic form, a neural network is composed of a sequence of layers, each containing multiple computational units (neurons). For each layer $l \in \{1, \dots, L\}$, let $h^{(l-1)}$ denote the input vector and $h^{(l)}$ the output vector. The layer computes an affine transformation followed by a nonlinear activation:

$$z^{(l)} = W^{(l)} h^{(l-1)} + b^{(l)}, \tag{5.4}$$

$$h^{(l)} = \phi^{(l)}\left(z^{(l)}\right), \tag{5.5}$$

where $z^{(l)}$ is the pre-activation vector, $W^{(l)}$ and $b^{(l)}$ are the weights and biases, and $\phi^{(l)}(\cdot)$ is the element-wise nonlinear activation (e.g., ReLU, tanh, or sigmoid) that produces the later output $h^{(l)}$. Model parameters are learned by minimizing a loss function that measures the mismatch between predicted outputs and ground-truth targets, typically using gradient-based optimization methods such as gradient descent [111].

Neural networks are widely used for short-term forecasting because they can learn nonlinear relationships and complex temporal patterns directly from data, without requiring an explicit physical model of the underlying process. In this context, forecasting is commonly formulated as a supervised learning problem, where model parameters are learned from examples pairing past observations (and other available information) with future values to be predicted [109, 110]. From a high-level perspective, neural network-based forecasting models implement a mapping from a finite history of measurements (often complemented by additional known descriptors, e.g., time-related variables) to one-step-ahead or multi-step predictions over a short horizon [112, 113].

Different neural network architectures instantiate this mapping in different ways. The most common families for time-series forecasting include recurrent models (e.g., LSTM-based) and attention-based models (e.g., Transformers) [114, 115]. Convolutional and feed-forward architectures are also widely used as competitive alternatives for short-term prediction [113]. The next subsections provide a concise overview of these model families, with emphasis on recurrent and attention-based architectures.

Recurrent Neural Networks and LSTM

Recurrent neural networks (RNNs) are a family of neural networks designed to process sequential data by maintaining a hidden state that is updated as new elements of the sequence are observed [110]. This recursive structure makes RNNs a common choice for time-series forecasting, where predictions depend on both recent and more distant past measurements. In practice, however, standard RNNs may suffer from training difficulties when modeling long-range dependencies, mainly due to vanishing and exploding gradient effects [116].

RNNs provide a compact way to summarize a history window into a state representation and are often effective when the relevant dynamics are captured by recent past information. A key drawback is that sequence processing is inherently sequential, which limits parallelization and can increase training and inference time compared to non-recurrent architectures [110].

Long Short-Term Memory (LSTM) neural networks are a specific type of RNN designed to alleviate these cited limitations by augmenting the *hidden state*—a compact internal representation that summarizes relevant information from past inputs—with an explicit memory (the *cell state*) and *gated* update mechanisms [114]. In other words, LSTM belongs to the RNN family because it processes sequences recurrently, but it differs from standard RNNs in how information is propagated over time. At each time step, the LSTM uses three gates, which can be interpreted as data-dependent filters: the *forget gate* decides which part of the previous memory should be retained or discarded, the *input gate* determines how much new information should be written into memory, and the *output gate* controls how much of the stored memory should be exposed to produce the current hidden state [114]. By explicitly regulating information flow in this way, LSTM can preserve relevant content over longer time spans and mitigate gradient-related issues during training, which has made them one of the widely adopted baselines in many short-term forecasting applications [113].

The main advantages of LSTMs are their improved ability to capture longer temporal dependencies and their generally more robust training behavior compared to standard RNNs. These benefits come at the cost of increased model complexity (more parameters and higher computational effort), and performance may still degrade when very long time windows are required or when training data are limited [113].

Hybrid LSTM Variants

Hybrid LSTM models denote a broad class of forecasting architectures that combine an LSTM block—used to encode temporal dependencies from a sequence of past observations—with additional components designed to exploit complementary information sources. The main motivation is that short-term forecasting often benefits from jointly capturing both sequential patterns in the recent history and contextual descriptors that are not naturally represented as a pure sequence [113].

A hybrid LSTM architecture of this type is adopted in Paper A, following the structure proposed in [117].

A common hybrid structure processes the historical time window through one or more LSTM layers to obtain a representation of the recent dynamics, which is then concatenated with auxiliary inputs (e.g., time-related descriptors or other available variables). The resulting feature vector is finally mapped to the forecast through a dense neural network. This design can be interpreted as a two-branch architecture: a *sequence branch* that extracts temporal features and a *context branch* that provides additional predictors, followed by a final fusion stage [117].

Attention-Based Models and Transformers

Attention-based models have recently become prominent in sequence modeling by enabling a neural network to focus on the most relevant parts of its input when forming a prediction [118]. Unlike recurrent architectures, which propagate information through a step-by-step state update, attention mechanisms operate by computing data-dependent interactions between elements of the input sequence, thereby providing a flexible way to represent temporal dependencies.

The Transformer architecture is the most widely used attention-based model family. Its core building block is *self-attention*, where each element of the input sequence is represented by attending to (i.e., forming weighted combinations of) all other elements in the sequence. Conceptually, this allows the model to capture both short- and long-range dependencies without relying on a recurrent state. Because self-attention can be implemented using highly parallel matrix operations, Transformer models are often more responsive to parallelization during training than RNN-based architectures [115].

A Transformer-based forecasting model of this type, following the architecture proposed in [115], is adopted in Paper B.

For time-series forecasting, Transformer-based models are commonly applied by representing a fixed history window (optionally augmented with additional covariates) as a sequence of tokens. Since the Transformer does not inherently encode the ordering of the sequence, temporal position information is typically provided through *positional encodings* [115]. The model then maps the input sequence representation to one-step-ahead or multi-step predictions, either directly or through recursive evaluation [113].

Transformer models are attractive in forecasting applications due to their ability to model complex dependencies and their favorable computational properties on modern hardware. On the other hand, they typically require careful design choices and tuning (e.g., number of layers/heads, regularization) and may require more data than simpler recurrent baselines [110].

Other Common Model Families

Besides recurrent and attention-based architectures, several other neural network families are commonly used for short-term time-series forecasting. The simplest and widely adopted baseline is the feed-forward (fully connected) neural network. In this case, the input is typically a fixed-length vector built from recent past measurements, possibly augmented with additional available descriptors, which is then mapped to the forecast through a sequence of dense layers [110]. Despite their simplicity, these models can be competitive when the forecast horizon is short and the relevant dynamics are largely captured by recent history.

Convolutional neural networks (CNNs) and related temporal convolutional architectures provide an alternative way to model sequential data. These models can be used to capture local temporal patterns and, when combined with multiple layers, can represent dependencies across larger time scales while maintaining favorable computational properties [110]. In forecasting applications, convolutional models are often used either as standalone predictors or as feature-extraction blocks preceding other components.

Finally, hybrid combinations of the above families are frequently encountered in practice. For example, convolutional layers can be used to extract short-term patterns before a recurrent module, or simple feed-forward branches can be used to incorporate auxiliary descriptors alongside a temporal encoder [113]. Overall, the choice among these model families is typically guided by the characteristics of the data, the desired forecasting horizon, and practical considerations such as computational cost and ease of training.

CHAPTER 6

Vehicle-Home-Grid-PV Control

This chapter introduces the control layer that integrates the component models discussed in the previous chapters into a single, operational energy management strategy. While Chapters 2–5 presented the main building blocks of this work in isolation, such as bidirectional charging, battery degradation modeling, PV generation modeling, and the treatment of uncertainty in future household demand and PV generation, here the focus shifts to how these elements are combined within a unified Vehicle–Home–Grid–PV (VHGPV) system and coordinated through a real-time controller. The goal is to compute charging/discharging and power exchange decisions online, while enforcing technical limits and user-centric requirements, and exploiting the available flexibility to reduce operating costs without inducing excessive battery degradation.

The chapter is organized as follows. Section 6.1 describes the VHGPV control problem and the adopted operating modes, i.e., parking and driving modes. Section 6.2 introduces the proposed MPC-based control strategy, with particular emphasis on the shrinking-horizon implementation tailored to finite parking intervals. Finally, Section 6.3 briefly reviews other control approaches that could be adopted for similar energy management problems.

6.1 VHGPV Operation and Control Problem

This section describes the real-time energy management problem considered in this thesis and summarizes the operating modes adopted for the VHGPV system. The considered scenario consists of a single EV and a single household equipped by bidirectional charger, and the electric grid. In addition, rooftop PV generation is included as an on-site renewable source (as in Paper B). The resulting VHGPV configuration is illustrated in Fig. 6.1.

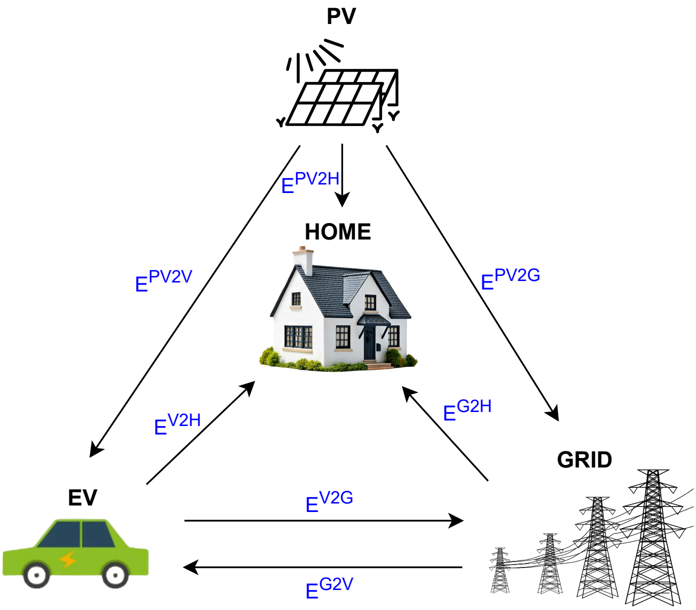

Figure 6.1: The proposed Vehicle-home-grid-PV configuration. The arrows indicate the allowable energy flows for V2G, V2G, G2V, G2H, PV2V, PV2H and PV2G.

As shown in the figure, the EV can supply energy to both the grid and the household, enabling Vehicle-to-Grid (V2G) and Vehicle-to-Home (V2H) operation, while Grid-to-Vehicle (G2V) represents conventional EV charging. The household can also be supplied directly from the grid through the standard Grid-to-Home (G2H) flow. PV generation can be self-consumed by the household load (PV2H), used to charge the EV (PV2V), and, when surplus energy is available, exported to the grid (PV2G). Throughout this work, it is assumed that the EV can be charged only when parked at home; therefore, public charging stations are not considered.

Operating Modes: Driving Versus Parking

The controller accounts for the fact that the EV alternates between two different operating modes, reflecting real-world operation.

Driving mode. When the EV is driving and therefore disconnected from the home charger, it cannot participate in energy exchange. In this mode, no optimization is performed and the system follows a simple rule-based logic, since the EV cannot exchange power with the household or the grid. Specifically, the household load is supplied by PV generation whenever available; any remaining demand is met by importing energy from the grid. Conversely, if PV production exceeds the household demand, the surplus is exported to the grid. During driving, the EV state-of-energy (SoE) (equivalent to SoC, as specified in Section 3.3) decreases according to the mobility energy consumption, considering the assumption that the EV is only charged at home.

Parking mode. When the EV is parked at home and connected to the bidirectional charger, it becomes an active energy storage that can be charged from the grid or PV and, if enabled, can supply energy to the household and/or export to the grid (V2H/V2G). In this mode, the controller computes optimal set-points by solving a constrained optimization problem in a receding-horizon fashion (Section 6.2), to determine the charging/discharging power and the grid exchange that best satisfy the control objectives. Decisions are updated every hour using the latest battery state measurement and updated predictions for the exogenous variables.

This separation reflects a realistic operational assumption: flexibility is only available during home parking intervals, which are the time windows in which real-time energy management is performed.

Exogenous Inputs and Forecast Horizon

A key challenge arises from uncertainty in the exogenous variables that drive the optimal decisions. In particular, future household demand and PV generation are not known in advance and are therefore predicted, as discussed in Chapter 5. This uncertainty is irrelevant when the EV is driving, since no optimization is performed and the EV is not available for energy exchange. In contrast, when the EV is parked and connected to the bidirectional charger, forecasts are required because the controller must anticipate future demand and PV availability to schedule EV charging and discharging actions, and power exchanging. In this case, the prediction horizon is aligned with the parking window: if the EV is expected to remain connected for T_p hours, the controller relies on forecasts covering the next T_p time steps, combining the current measured values with predictions for the remaining hours. As time progresses, the remaining parking time decreases and the optimization horizon is updated accordingly, which motivates the use of a shrinking-horizon MPC formulation (Section 6.2).

Objectives and Constraints

The primary objective of this work is to minimize the user's operating cost over the simulated period. In particular, the controller is designed to minimize both the electricity cost associated with energy imported from and exported to the grid under time-varying prices, and the cost associated with EV battery degradation induced by charging/discharging operation. In compact form, this total cost can be expressed as

$$C_{tot} = C_{\text{energy}} + C_{\text{degradation}}, \tag{6.1}$$

where C_{energy} denotes the electricity cost and $C_{\text{degradation}}$ denotes the battery degradation-related cost. The degradation term is quantified through the aging model introduced in Chapter 3 and converted into a monetary cost following economic principles discussed in [119], so that both cost contributions are expressed in the same unit and can be jointly optimized within a single objective function. Regarding the energy-related term C_{energy}, during parking mode it can be written as

$$C_{\text{energy}} = C_{\text{buy}} - R_{\text{sell}}, \tag{6.2}$$

where C_{buy} denotes the cost incurred by purchasing electricity from the public grid, and R_{sell} denotes the revenue obtained by exporting electricity to the grid (hence the minus sign in the total balance). These two contributions can be further decomposed as

$$C_{\text{buy}} = C_{\text{G2V}} + C_{\text{G2H}}, \tag{6.3}$$

$$R_{\text{sell}} = R_{\text{V2G}} + R_{\text{PV2G}}, \tag{6.4}$$

where C_{G2V} and C_{G2H} are the costs associated with grid energy used to charge the EV and to supply the household demand, respectively, while R_{V2G} and R_{PV2G} are the revenues obtained by exporting energy to the grid through EV discharging (V2G) and by selling surplus PV generation (PV2G). For further details on these formulations and the adopted pricing assumptions, the reader is referred to Paper A and Paper B.

It is important to note that this formulation is *passive* during driving mode: when the EV is disconnected, no optimization problem is solved and the cost simply accumulates according to the realized energy exchanges (i.e., the household being supplied by PV and/or the grid) and the EV mobility consumption. In this case, the expressions for C_{buy} and R_{sell} reduce to

$$C_{\text{buy}} = C_{\text{G2H}}, \tag{6.5}$$

$$R_{\text{sell}} = R_{\text{PV2G}}, \tag{6.6}$$

since the EV is not available and therefore cannot be charged from the grid nor discharge to support the household or export to the grid. In contrast, the formulation becomes *active* during parking mode, when the EV is connected and controllable. In this case, the cost in (6.1) defines the objective to be minimized, and the controller explicitly optimizes the charging/discharging set-points and the grid power exchange to reduce the predicted total cost, leveraging forecasts of household demand and PV production.

The optimization problem is subject to both technical and user-centric constraints. Technical constraints include charger power limits for EV charging and discharging, bounds on the admissible EV SoE, and (when applicable) limits on the net power exchanged with the grid. User-centric constraints are included to preserve mobility needs and mitigate range anxiety, for instance by enforcing a minimum SoE level (either at departure or over portions of the parking interval) to ensure sufficient energy availability for unexpected trips. Further details on the adopted constraints are provided in Paper A and Paper B. Together, these constraints ensure that economic optimization does not compromise system feasibility, hardware limitations, or the EV's primary transportation function.

6.2 Model Predictive Control for Bidirectional Charging

Model Predictive Control (MPC) is an optimization-based control framework in which control actions are obtained by repeatedly solving a finite-horizon optimal control problem in real time [30]. MPC is widely adopted for the control of constrained energy systems because it can enforce operational limits (e.g., power bounds and state constraints) while leveraging predictions of future exogenous inputs (e.g., demand and renewable generation). At each time step, MPC uses a predictive model of the system to evaluate how candidate decisions affect future states and costs, and selects the control action that achieves the best trade-off between economic performance and technical feasibility under time-varying operating conditions.

Receding-Horizon Concept

The defining feature of MPC is the receding-horizon (or moving-horizon) implementation. At each discrete time step k, the controller formulates and solves a finite-horizon constrained optimization problem using the most recent information available at time k (e.g., current battery SoE and current measurements of demand/PV), and forecasts of the relevant exogenous quantities over the next N steps. The decision variables are the planned control actions over the horizon, i.e.,

$$u(k|k),\ u(k+1|k),\ \ldots,\ u(k+N-1|k),$$

which typically represent charging/discharging and power exchange set-points. These decision variables are chosen to minimize a cumulative objective (in our case, energy cost and degradation cost) while satisfying all constraints over the horizon. Importantly, feasibility over the horizon is enforced by including the system coupling relations (e.g., the energy balance linking SoE across time) and the relevant operational limits (e.g., SoE bounds and power limits).

Once the optimization is solved, only the first element of the optimal plan, $u(k|k)$, is implemented. At the next time step $k+1$, new measurements become available and the forecasts are updated; the optimization problem is then solved again over a horizon shifted one step ahead. In this way, MPC produces a sequence of decisions through repeated re-optimization, allowing the controller to continuously adapt to forecast errors and changing operating conditions while still optimizing performance over a look-ahead window.

Shrinking-Horizon MPC

Shrinking-horizon MPC (SH-MPC) is a finite-horizon MPC implementation in which the prediction horizon length decreases over time, rather than remaining constant [120]. This differs from the standard receding-horizon implementation, where the horizon is shifted forward at each time step while its length N is typically kept fixed. In SH-MPC, the horizon is shifted forward as well, but its length is updated to match a finite remaining time window, so that the last prediction step is anchored to a fixed terminal time (in this case, a known departure time). Consequently, the number of decision variables and constraints decreases as the terminal time is approached.

This formulation is particularly appropriate for the VHGPV setting considered in this thesis because the EV is controllable only during home-parking intervals, which are inherently finite. Let t_a denote the plug-in (arrival) time step and t_p the expected pickup (departure) time step. At each time step within the parking interval, the optimization is carried out over the remaining controllable window, i.e., up to the departure time. Accordingly, the horizon length decreases as the pickup time approaches, and can be expressed conceptually as

$$N(k) = t_p - k + 1, \tag{6.7}$$

so that the optimization problem always spans the remaining time steps until departure, including the terminal step t_p.

In this context, SH-MPC brings two main advantages. First, it ensures that optimization is performed only over time intervals in which the EV is available for control. Second, it provides a direct way to handle departure-related requirements, such as enforcing a minimum SoE at t_p, or additional mobility constraints to mitigate range anxiety. Overall, SH-MPC retains the feedback nature of MPC through repeated re-optimization, while explicitly accounting for the finite and time-varying actuation window that characterizes home bidirectional charging.

Shrinking-Horizon MPC Formulation for VHGPV Control

In the VHGPV setting considered in this thesis, MPC is adopted during parking intervals, when the EV is connected and controllable. In particular, a SH-MPC implementation is used because control authority is available only over a finite home-parking window: once the pickup time is reached, the EV disconnects and no further charging/discharging decisions can be applied. Accordingly, at each hourly time step, the controller solves a constrained optimization problem over the remaining time-to-departure to determine the EV charging/discharging power and the net grid exchange that minimize the predicted total cost (energy cost plus degradation cost), using forecasts of household demand and PV generation and enforcing technical limits and mobility-related constraints. In this thesis, the resulting SH-MPC formulation is *deterministic*, as uncertainty in household demand and PV production is represented through point forecasts (obtained from the forecasting models in Chapter 5), rather than through uncertainty sets or probabilistic scenarios.

The controller operates with a sampling time of $\Delta t = 1$ h, and the time index t therefore refers to hourly intervals. Let $\bar{t}$ denote the present time step, and let us keep the notation of t_a and t_p to denote the EV plug-in (arrival) and pickup (departure) time steps, respectively. During a parking interval, the SH-MPC problem is solved at each $\bar{t} \in \{t_a, t_a + 1, \ldots, t_p\}$ over the remaining parking horizon $t = \bar{t}, \ldots, t_p$. Recalling (6.1), an implementation of the stage cost, consistent with the shrinking-horizon logic and aligned with the formulations adopted in Paper A and Paper B, is the following:

$$\min \sum_{t=\bar{t}}^{t_p} C_{\text{energy},t} + C_{\text{degradation},t}, \tag{6.8}$$

where the objective is written as a sum of per-step costs over the remaining parking window. More explicitly, at each $\bar{t}$ the optimization is carried out over the planned charging/discharging and grid-exchange set-points $\{u_t\}_{t=\bar{t}}^{t_p}$.

Energy-based discretization. Following the convention adopted throughout this thesis (and in Paper A and Paper B), decision variables are expressed in energy units (kWh) rather than power units (kW). With hourly discretization ($\Delta t = 1$ h), the energy exchanged over one interval satisfies $E_t = P_t \Delta t$, where P_t denotes the average power over the interval. Consequently, cost terms that depend on the exchanged electricity can be formulated either in terms of E_t

or $P_t \Delta t$. Since $\Delta t = 1$ h, E_t and P_t coincide numerically for each interval, and the energy-based notation is adopted for compactness.

6.3 Other Control Approaches for Real-Time Energy Management

Besides deterministic MPC-based strategies, there are alternative control approaches that can be used for real-time energy management. The overview below is concise and is included to place the deterministic SH-MPC approach adopted in this thesis within the broader set of real-time energy management methods.

Rule-Based and Heuristic Strategies

Rule-based and heuristic controllers implement predefined decision rules, typically based on thresholds and priorities [121] (e.g., "use PV to supply the household first, export surplus to the grid, and charge the EV when the price is low"). In this thesis, a rule-based logic is adopted during driving mode, when the EV is disconnected and no optimization is required: the household is supplied by PV whenever available, any deficit is covered by grid imports, and any PV surplus is exported to the grid. Such strategies are attractive due to their simplicity, low computational burden, and ease of implementation on embedded hardware. However, they generally do not provide optimality guarantees and can be difficult to tune when multiple, competing objectives are present (e.g., electricity cost, battery aging, and mobility constraints). In addition, their performance may degrade under changing operating conditions or tariff structures, since the rules must be redesigned or re-tuned to reflect new scenarios.

Robust and Stochastic MPC

The SH-MPC formulation adopted in this thesis is *deterministic*, in the sense that uncertainty in household demand and PV generation is represented through point forecasts. In contrast, uncertainty can be handled more explicitly within robust or stochastic MPC frameworks. Robust MPC seeks decisions that remain feasible for all realizations of disturbances within a prescribed uncertainty set, often at the cost of increased conservatism [122]. Stochastic MPC, instead, models uncertainty probabilistically and can incorporate chance constraints or expected-value objectives, potentially achieving less conservative operation when uncertainty statistics are available [123]. These approaches can improve reliability in the presence of large forecast errors, but increase computational complexity and require either accurate uncertainty sets (robust MPC) or reliable probabilistic models (stochastic MPC), which may not be readily available in practical residential settings.

Learning-Based Control (Reinforcement Learning)

Learning-based methods, and in particular Reinforcement Learning (RL), represent an alternative in which a control policy is learned from data and/or interaction with a simulation environment. RL is known to handle nonlinear dynamics and complex decision-making without relying on an explicit analytical model [124]. However, its direct application to energy management poses several practical challenges. First, enforcing hard operational constraints (e.g., SoE bounds and power limits) in a reliable way is nontrivial. Second, training typically requires substantial data and simulation design to cover relevant operating conditions. Third, performance and safety may degrade when the policy is deployed under conditions that differ from the training distribution (e.g., different tariffs, weather patterns, or user behavior). For these reasons, RL is often considered either in combination with constraint-handling mechanisms or as a complement to optimization-based approaches.

Optimization-Based Scheduling

Optimization-based scheduling computes a plan over a given horizon (e.g., a day ahead) by solving a deterministic optimization problem based on forecasts and operational constraints. In its basic form, the plan is computed once and then implemented in open loop, i.e., without repeated re-optimization at every sampling instant. This makes scheduling particularly suitable for offline or planning-oriented settings in which future inputs are assumed to be known in advance, and deviations are not expected [125].

When deviations do occur (e.g., due to unexpected events), a common practice is to augment the open-loop schedule with corrective actions, implemented through rule-based logic [126]. While such corrections can improve feasibility and practical performance, they do not generally preserve the optimality properties of the original schedule. It is worth noting that MPC can be formulated using the same underlying optimization models as scheduling; the key distinction lies in the implementation: MPC repeatedly resolves the optimization online using updated measurements and forecasts, thereby providing a closed-loop decision-making mechanism that is responsive to uncertainty and variability.

CHAPTER 7

Summary of Included Papers

This chapter provides a summary of the included papers.

7.1 Paper A

Francesco Popolizio, Torsten Wik, Chih Feng Lee and Changfu Zou
Online Aging-aware Energy Optimization for Vehicle-Home-Grid Integration
Submitted to *International Federation of Automatic Control (IFAC) World Congress*, Busan, Republic of Korea, Aug. 2026.

This paper studies the economic potential of vehicle–home–grid integration enabled by bidirectional charging, using an online optimization strategy that schedules power exchanges among an electric vehicle, a residential household, and the public grid. The controller leverages V2H to reduce grid imports and increase self-consumption, and V2G to exploit time-varying electricity prices through energy trading (arbitrage) when economically convenient. Since the household demand is not perfectly known in advance, the method operates in a receding/shrinking-horizon fashion over each home-parking interval, repeatedly re-optimizing the charging/discharging plan as updated load information becomes available. To support these online updates, the framework relies on a data-driven household load forecast based on a hybrid LSTM predictor. To evaluate the profitability of V2H and V2G under dynamic electricity prices, the framework also accounts for battery aging via a nonlinear model capturing both calendar and cycle degradation. The resulting optimization minimizes the total operating cost as the sum of electricity purchase/sale costs (with a V2G selling-price ratio) and an equivalent battery degradation cost that translates capacity fade into monetary terms via battery value and end-of-life assumptions. Year-long simulations show that bidirectional operation can yield substantial economic gains compared to unidirectional smart charging, while inducing only a limited additional aging impact. Moreover, even under unfavorable electricity selling conditions (low V2G selling-price ratio), V2H alone still provides consistent savings by shifting energy between the EV and the household. A sensitivity analysis further clarifies the operating regimes in which bidirectional services are most beneficial and quantifies the trade-off between cost reduction and battery wear.

Contributions: **Francesco Popolizio** contributed with conceptualization, methodology, software, data acquisition, validation, writing–original draft, review & editing. **Torsten Wik** contributed with writing–review & editing, supervision. **Chih Feng Lee** contributed with writing–review & editing, supervision. **Changfu Zou** contributed with writing–review & editing, supervision, funding acquisition.

7.2 Paper B

Francesco Popolizio, Albert Škegro, Torsten Wik, Chih Feng Lee and Changfu Zou
Online Energy Management for Bidirectional EV Charging with Rooftop PV: An Aging-Aware MPC Approach
Submitted to *IEEE Transactions on Transportation Electrification.*

Building on the previous study, this paper investigates the economic impact of residential vehicle–home–grid integration in the presence of rooftop PV by proposing an online, aging-aware energy management strategy for an electric vehicle, a household, and the electrical grid. The MPC framework explicitly exploits V2H and V2G operation to increase self-consumption and perform price-driven arbitrage, while respecting user-driven mobility requirements. Since both household demand and PV generation are not perfectly known in advance, power flows are optimized over each home-parking interval through a shrinking-horizon MPC scheme, re-optimized as updated measurements and forecasts become available. To support these online updates, the controller relies on a Transformer-based forecaster that provides short-term predictions of household load and solar irradiance (used to estimate PV generation). The controller incorporates a detailed nonlinear battery aging model, capturing both calendar and cycle degradation, which is subsequently linearized for tractable optimization. The optimization minimizes the total operating cost by combining electricity purchase/sale costs (parameterized by a V2G selling-price ratio) with an equivalent battery degradation cost that monetizes capacity fade. The study evaluates two configurations: a vehicle–home–grid system without PV and an extended vehicle–home–grid–PV setup. A one-year case study under Swedish conditions shows that the proposed strategy achieves the lowest annual cost among the considered strategies. Adding rooftop PV increases the annual profit by €1060.7 compared to operating without PV, and bidirectional operation can provide an economic gain of up to €2410.5 over smart unidirectional charging, at the expense of only 1.27% additional battery degradation. Even in the least favorable case with no remuneration for exported V2G energy, bidirectional operation remains beneficial: V2H alone still delivers €355.8 annual savings with negligible extra wear. Sensitivity analyses over V2G price ratio, EV battery size, household demand, and pickup time uncertainty confirm that these benefits persist across a wide range of scenarios, with larger batteries generally being better suited for bidirectional services.

Contributions: **Francesco Popolizio** contributed with conceptualization, methodology, software, data acquisition, validation, writing–original draft, review & editing. **Albert Škegro** contributed with validation, writing–original draft, review & editing. **Torsten Wik** contributed with writing–review & editing, supervision. **Chih Feng Lee** contributed with writing–review & editing, supervision. **Changfu Zou** contributed with writing–review & editing, supervision, funding acquisition.

CHAPTER 8

Concluding Remarks and Future Work

This thesis investigated how bidirectional charging can be exploited to integrate an EV into a residential energy system as an active flexibility resource, enabling both V2H and V2G operation, optionally in the presence of rooftop PV generation. Driven by the rapid growth of EVs, a key motivation is that private cars remain parked for most of the day and therefore represent an underutilized source of flexibility. When equipped with bidirectional chargers, EVs can support local energy balancing, increase household self-consumption, especially in PV-equipped homes, by shifting surplus PV generation to later demand, and export electricity to the grid to exploit time-varying prices through price-driven arbitrage. When managed appropriately, these capabilities can reduce the user's annual electricity cost, while still satisfying mobility requirements.

A crucial barrier to widespread adoption, however, is users' concern about accelerated battery aging due to the additional cycling required by V2H and V2G services. To study this trade-off, this thesis developed an online control framework based on an SH-MPC scheme. During each home-parking interval, power flows among the EV, household, grid, and PV system are optimized while enforcing operational constraints and user-driven mobility needs. During driving mode, instead, the EV is disconnected and therefore cannot participate in energy management. In this case, the residential system is handled through a simple rule-based logic that regulates the power exchange between the household, the PV system, and the grid.

A challenge is that future household demand and PV production are not known in advance, so the controller cannot rely on perfectly known trajectories over the prediction horizon. To address this, the SH-MPC scheme is coupled with a neural-network-based forecaster that provides short-term estimates of the required quantities. The optimization is then re-solved at each time step as new measurements become available, updating the plan online to limit the impact of forecast errors.

Battery lifetime effects are explicitly accounted for through semi-empirical degradation models that combine calendar aging and cycle aging. By including the associated wear cost in the optimization, the controller can trade off electricity-cost savings (or arbitrage revenues) against battery degradation, enabling an aging-aware exploitation of bidirectional charging.

Overall, the results in Paper A and Paper B—which directly address the research questions posed in Section 1.1—confirm that treating an EV as an active energy node and enabling V2G and V2H through the proposed controller can consistently reduce the user's electricity cost across the considered scenarios. Notably, even V2H-only operation delivers clear benefits by shifting energy to avoid expensive grid imports. At the same time, the battery aging associated with bidirectional operation remains limited, ranging from negligible to modest in the tested cases. Sensitivity analyses further indicate that these conclusions are robust under different operating conditions, and show that larger-capacity batteries are particularly well-suited for bidirectional services, as they can provide greater flexibility and savings while keeping degradation at acceptable levels.

Future Work

While the proposed framework and the results in Paper A and Paper B provide clear evidence of the potential of residential V2G and V2H operation, several directions remain open for further research.

A first direction is to evaluate the generalizability of the proposed framework and the role of battery aging in the overall economic model. This requires testing the controller under alternative market and regulatory conditions (e.g., different countries/cities, tariff structures, taxes, and incentive schemes) and with diverse datasets for household demand, PV generation, and driving patterns. Such cross-case evaluation would clarify how sensitive the economic conclusions are to local price signals and user behavior, and to what extent battery degradation remains a dominant (or secondary) driver of the optimal strategy. Moreover, it would help identify which parameters and modeling assumptions most strongly affect the predicted aging and its monetized impact, thereby improving the robustness and transferability of the proposed approach.

Another extension is to move from a single-user setting to a multi-user and aggregation-based control. Coordinating multiple residential EV–home systems would enable the study of collective benefits, fairness among users, and the emergence of new constraints at the community level. Importantly, once multiple self-interested users are considered, conflicts of interest may arise: strategies that are individually optimal can become harmful at the system level, potentially creating new congestion patterns (e.g., synchronized charging/discharging) and shifting stress to different hours or network locations.

A closely related direction is to shift the perspective from user-centric cost minimization to grid-centric objectives, exploiting bidirectional charging to provide grid services such as peak shaving, frequency support, congestion management, and flexibility provision. While recent developments already point to the feasibility of EV-based flexibility at scale, an open challenge is how to coordinate large numbers of small residential "micro-ecosystems" (EV–home–PV) in a way that is scalable, robust to uncertainty, and compatible with distribution-network constraints, so that bidirectional charging becomes not only economically attractive for users, but also a reliable resource for supporting the power system.

A further direction is grid resilience. As distribution systems face increasing stress from electrification, higher peaks, and more variable renewable generation, maintaining secure operation is essential not only for economic efficiency but also for security of supply. In this context, bidirectional charging can act as a distributed resilience resource: in normal operation, coordinated V2G and V2H may mitigate peaks and preserve operational margins; during faults or outages, EV batteries could support critical loads and assist restoration. Future work should develop resilience-oriented control formulations to coordinate many residential EV–home–PV systems while respecting mobility requirements and battery aging limits.

From a control perspective, especially when extending the framework to a multi-user setting, it would be valuable to investigate robust and stochastic MPC formulations that explicitly account for uncertainty rather than relying solely on neural-network point forecasts. By incorporating uncertainty sets or scenario-based representations, the controller could make decisions that remain reliable under forecast errors and user interactions.

Finally, a key step to strengthen the practical relevance of these research directions is to validate the proposed concepts under more realistic assumptions and operating conditions, including high-fidelity component models and, where possible, experimental or pilot-based testing. Such validation would help quantify performance and scalability in real-world operation, and clarify the requirements for translating residential bidirectional control from simulation studies to deployable energy management solutions.

References

[1] International Energy Agency, *Global EV Outlook 2024*, IEA Report (online), Licence: CC BY 4.0, Paris, 2024. [Online]. Available: https://www.iea.org/reports/global-ev-outlook-2024.

[2] International Energy Agency, *Global EV Outlook 2025*, IEA Report (online), Licence: CC BY 4.0, Paris, 2025. [Online]. Available: https://www.iea.org/reports/global-ev-outlook-2025.

[3] Benchmark Mineral Intelligence, *Global EV sales reach 20.7 million units in 2025, growing by 20%*, Benchmark Source (Benchmark Mineral Intelligence), Accessed: 2026-01-20, Jan. 2026. [Online]. Available: https://source.benchmarkminerals.com/article/global-ev-sales-reach-20-7-million-units-in-2025-growing-by-20.

[4] UNFCCC, *Paris agreement*, United Nations Framework Convention on Climate Change (UNFCCC), Accessed: 2026-01-20, 2015. [Online]. Available: https://unfccc.int/sites/default/files/english_paris_agreement.pdf.

[5] International Energy Agency, *Energy efficiency 2025: Transport*, IEA Report (online), Licence: CC BY 4.0., Paris, 2025. [Online]. Available: https://www.iea.org/reports/energy-efficiency-2025/transport.

[6] International Energy Agency, *Electricity 2025: Demand*, IEA Report (online), Licence: CC BY 4.0., Paris, 2025. [Online]. Available: https://www.iea.org/reports/electricity-2025/demand.

[7] International Energy Agency, *Renewables 2025*, IEA Report (online), Licence: CC BY 4.0., Paris, 2025. [Online]. Available: https://www.iea.org/reports/renewables-2025.

[8] G. Barbose and A. Satchwell, "Benefits and costs of a utility-ownership business model for residential rooftop solar photovoltaics," *Nature Energy*, vol. 5, pp. 750–758, 2020. [Online]. Available: https://doi.org/10.1038/s41560-020-0673-y.

[9] S. Han, S. Han, and K. Sezaki, "Development of an optimal vehicle-to-grid aggregator for frequency regulation," *IEEE Transactions on Smart Grid*, vol. 1, no. 1, pp. 65–72, 2010.

[10] P. Kou, D. Liang, L. Gao, and F. Gao, "Stochastic coordination of plug-in electric vehicles and wind turbines in microgrid: A model predictive control approach," *IEEE Transactions on Smart Grid*, vol. 7, no. 3, pp. 1537–1551, 2016.

[11] M. D. Dean and K. M. Kockelman, "Assessing Public Opinions of and Interest in Bidirectional Electric Vehicle Charging Technologies: A U.S. Perspective," *Transportation Research Record*, vol. 2678, no. 12, pp. 1889–1904, 2024. [Online]. Available: https://doi.org/10.1177/03611981241253608.

[12] J. Bakhuis, N. Barbour, and É. J. L. Chappin, "Exploring user willingness to adopt vehicle-to-grid (V2G): A statistical analysis of stated intentions," *Energy Policy*, vol. 203, p. 114 619, 2025.

[13] G. Santinha and J. Tavares, "A systematic review of citizen perceptions and expectations of v2g adoption in the context of sustainable transitions," *Discover Sustainability*, vol. 6, p. 957, Sep. 2025.

[14] J. Einolander, A. Kiviaho, and R. Lahdelma, "Valuing the household power outage self-sustainment capabilities of bidirectional electric vehicle charging," *Applied Energy*, vol. 374, p. 124 071, Nov. 2024.

[15] R. Khezri, D. Steen, and A. T. Le, "Willingness to Participate in Vehicle-to-Everything (V2X) in Sweden, 2022—Using an Electric Vehicle's Battery for More Than Transport," *Sustainability*, vol. 16, no. 5, p. 1792, 2024.

[16] Y. Wu, S. M. Aziz, and M. H. Haque, “Vehicle-to-home operation and multi-location charging of electric vehicles for energy cost optimisation of households with photovoltaic system and battery energy storage,” *Renewable Energy*, vol. 221, p. 119 729, Feb. 2024.

[17] D. Gudmunds, E. Nyholm, M. Taljegård, and M. Odenberger, “Self-consumption and self-sufficiency for household solar producers when introducing an electric vehicle,” *Renewable Energy*, vol. 148, pp. 1200–1215, Apr. 2020.

[18] T. Kern, P. Dossow, and E. Morlock, “Revenue opportunities by integrating combined vehicle-to-home and vehicle-to-grid applications in smart homes,” *Applied Energy*, vol. 307, p. 118 187, Feb. 2022.

[19] S. Mohseni and A. C. Brent, “Co-optimization of the sizing and dispatch of microgrids considering vehicle-to-grid and arbitrage,” in *2022 IEEE PES 14th Asia-Pacific Power and Energy Engineering Conference (APPEEC)*, 2022, pp. 1–7.

[20] S. Sagaria, M. van der Kam, and T. Boström, “The influence of socio-technical variables on vehicle-to-grid technology,” *Energy*, vol. 305, p. 132 299, 2024.

[21] F. Liu, Z. Wei, Y. Lin, X. Huang, Y. Li, Y. Huang, and M. K. Lim, “Vehicle-to-grid technology acceptance for electric vehicle users: A systematic literature review and future research agenda,” *International Journal of Consumer Studies*, vol. 49, no. 3, e70065, 2025.

[22] M. Ebrahimi, M. Rastegar, M. Mohammadi, A. Palomino, and M. Parvania, “Stochastic Charging Optimization of V2G-Capable PEVs: A Comprehensive Model for Battery Aging and Customer Service Quality,” *IEEE Transactions on Transportation Electrification*, vol. 6, no. 3, pp. 1026–1034, 2020.

[23] A.-H. Mohsenian-Rad and A. Leon-Garcia, “Optimal residential load control with price prediction in real-time electricity pricing environments,” *IEEE Transactions on Smart Grid*, vol. 1, no. 2, pp. 120–133, 2010.

[24] C.-F. Lu, G.-P. Liu, Y. Yu, and J. Cui, “A coordinated model predictive control-based approach for vehicle-to-grid scheduling considering range anxiety and battery degradation,” *IEEE Transactions on Transportation Electrification*, vol. 11, no. 2, pp. 5688–5699, 2025.

[25] W. Shi and V. W. Wong, "Real-time vehicle-to-grid control algorithm under price uncertainty," in *2011 IEEE International Conference on Smart Grid Communications (SmartGridComm)*, 2011, pp. 261–266.

[26] C. Hutson, G. K. Venayagamoorthy, and K. A. Corzine, "Intelligent scheduling of hybrid and electric vehicle storage capacity in a parking lot for profit maximization in grid power transactions," in *2008 IEEE Energy 2030 Conference*, 2008, pp. 1–8.

[27] M. Naumann, F. B. Spingler, and A. Jossen, "Analysis and modeling of cycle aging of a commercial LiFePO4/graphite cell," *Journal of Power Sources*, vol. 451, p. 227 666, 2020. [Online]. Available: `https://www.sciencedirect.com/science/article/pii/S0378775319316593`.

[28] C. F. Lee, K. Bjurek, V. Hagman, Y. Li, and C. Zou, "Vehicle-to-grid optimization considering battery aging," *IFAC-PapersOnLine*, vol. 56, no. 2, pp. 6624–6629, 2023.

[29] S. Sagaria, M. van der Kam, and T. Boström, "Vehicle-to-grid impact on battery degradation and estimation of v2g economic compensation," *Applied Energy*, vol. 377, p. 124 546, 2025.

[30] J. B. Rawlings, D. Q. Mayne, and M. M. Diehl, *Model Predictive Control: Theory, Computation, and Design*, 2nd ed. Nob Hill Publishing, 2017.

[31] O. Dankar, M. Tarnini, A. El Ghaly, N. Moubayed, and K. Chahine, "A neural network-based model predictive control for a grid-connected photovoltaic–battery system with vehicle-to-grid and grid-to-vehicle operations," *Electricity*, vol. 6, no. 2, p. 32, 2025.

[32] Polestar. "Home charging with polestar energy," Accessed: Jan. 22, 2026. [Online]. Available: `https://www.polestar.com/uk/charging/home-charging/`.

[33] K. M. Tan, V. K. Ramachandaramurthy, and J. Y. Yong, "Integration of electric vehicles in smart grid: A review on vehicle to grid technologies and optimization techniques," *Renewable and Sustainable Energy Reviews*, vol. 53, pp. 720–732, 2016.

[34] S. Habib, M. Kamran, and U. Rashid, "Impact analysis of vehicle-to-grid technology and charging strategies of electric vehicles on distribution networks — a review," *Journal of Power Sources*, vol. 277, pp. 205–214, 2015.

[35] Y. Zheng, S. Niu, Y. Shang, Z. Shao, and L. Jian, "Integrating plug-in electric vehicles into power grids: A comprehensive review on power interaction mode, scheduling methodology and mathematical foundation," *Renewable and Sustainable Energy Reviews*, vol. 112, pp. 424–439, 2019.

[36] X. Fang, S. Misra, G. Xue, and D. Yang, "Smart grid — the new and improved power grid: A survey," *IEEE Communications Surveys & Tutorials*, vol. 14, no. 4, pp. 944–980, 2012.

[37] V. C. Gungor, D. Sahin, T. Kocak, S. Ergut, C. Buccella, C. Cecati, and G. P. Hancke, "Smart Grid Technologies: Communication Technologies and Standards," *IEEE Transactions on Industrial Informatics*, vol. 7, no. 4, pp. 529–539, 2011.

[38] J. Burger, J. Hildermeier, A. Jahn, and J. Rosenow, "The time is now: Smart charging of electric vehicles," Regulatory Assistance Project (RAP), Tech. Rep., Apr. 2022, Report. [Online]. Available: `https://www.raponline.org/wp-content/uploads/2023/09/rap-jb-jh-smart-charging-europe-2022-april-26.pdf`.

[39] F. Brockmann and M. Guajardo, "Electric vehicle charging costs and power losses under the energy price crisis: Shifting dynamics in norway," *Energy Economics*, vol. 153, p. 109 052, 2026.

[40] A. Wallberg, C. Flygare, R. Waters, and V. Castellucci, "Peak shaving for electric vehicle charging infrastructure—a case study in a parking garage in uppsala, sweden," *World Electric Vehicle Journal*, vol. 13, no. 8, p. 152, 2022.

[41] J. Leijon, "Charging strategies and battery ageing for electric vehicles: A review," *Energy Strategy Reviews*, vol. 57, p. 101 641, 2025.

[42] T. M. Ngoc Bui, T. Q. Dinh, and J. Marco, "A study on electric vehicle battery ageing through smart charge and vehicle-to-grid operation," in *2021 24th International Conference on Mechatronics Technology (ICMT)*, 2021, pp. 1–7.

[43] B. K. Sovacool, J. Axsen, and W. Kempton, “The Future Promise of Vehicle-to-Grid (V2G) Integration: A Sociotechnical Review and Research Agenda,” *Annual Review of Environment and Resources*, vol. 42, pp. 377–406, 2017.

[44] M. A. Rehman, M. Numan, H. Tahir, U. Rahman, M. W. Khan, and M. Z. Iftikhar, “A comprehensive overview of vehicle to everything (v2x) technology for sustainable ev adoption,” *Journal of Energy Storage*, vol. 74, p. 109 304, 2023.

[45] C. Gschwendtner, S. R. Sinsel, and A. Stephan, “Vehicle-to-X (V2X) implementation: An overview of predominate trial configurations and technical, social and regulatory challenges,” *Renewable and Sustainable Energy Reviews*, vol. 145, p. 110 977, 2021.

[46] W. Kempton and J. Tomić, “Vehicle-to-grid power fundamentals: Calculating capacity and net revenue,” *Journal of Power Sources*, vol. 144, no. 1, pp. 268–279, 2005.

[47] C. Guille and G. Gross, “A conceptual framework for the vehicle-to-grid (v2g) implementation,” *Energy Policy*, vol. 37, no. 11, pp. 4379–4390, 2009.

[48] F. Mwasilu, J. J. Justo, E.-K. Kim, T. D. Do, and J.-W. Jung, “Electric vehicles and smart grid interaction: A review on vehicle to grid and renewable energy sources integration,” *Renewable and Sustainable Energy Reviews*, vol. 34, pp. 501–516, 2014.

[49] ISO, *ISO 15118-20:2022 Road vehicles — Vehicle to grid communication interface — Part 20: 2nd generation network layer and application layer requirements*, Edition 1, 2022-04, International Organization for Standardization, 2022.

[50] European Alternative Fuels Observatory (EAFO), “Pricing of electric vehicle recharging in europe,” European Commission, Tech. Rep., 2022, Report describing public recharging pricing structures.

[51] FIA Region I and Ricardo, “Public EV Charging in Europe: Market Dynamics and Consumer Perspectives,” FIA Region I, Tech. Rep., 2025, Report discussing common pricing models and market dynamics in public EV charging.

[52] K. Li, X. Li, Z. Xiong, S. Tao, G. Zhao, Y. Jiang, H. Qi, and Y. Zhang, "Unlocking vehicle-to-grid potential of load shifting in china's megacities considering comprehensive real-world behaviors," *Nature Communications*, vol. 16, no. 1, p. 10 087, 2025.

[53] ENTSO-E, *Frequency ranges (ENTSO-E guidance document)*, Technical document, Refers to 50 Hz nominal system and frequency ranges in Continental Europe, 2018.

[54] North American Electric Reliability Corporation (NERC), *Balancing and frequency control*, Technical reference document, Refers to 60 Hz nominal system and frequency ranges in North America, 2021.

[55] C. O'Malley, L. Badesa, F. Teng, and G. Strbac, "Frequency Response From Aggregated V2G Chargers With Uncertain EV Connections," *IEEE Transactions on Power Systems*, vol. 38, no. 4, pp. 3543–3556, 2023.

[56] M. M. Mattos, J. A. G. Archetti, L. d. A. Bitencourt, A. Wallberg, V. Castellucci, B. H. Dias, and J. G. de Oliveira, "Analysis of voltage control using v2g technology to support low voltage distribution networks," *IET Generation, Transmission & Distribution*, vol. 18, no. 6, pp. 1133–1157, 2024. [Online]. Available: `https://ietresearch.onlinelibrary.wiley.com/doi/abs/10.1049/gtd2.13066`.

[57] D. Dreucci, Y. Yu, G. R. Chandra Mouli, A. Shekhar, and P. Bauer, "Centralised distribution grid congestion management through ev charging control considering fairness and priority," *Applied Energy*, vol. 384, p. 125 417, 2025. [Online]. Available: `https://www.sciencedirect.com/science/article/pii/S0306261925001473`.

[58] U. Knight, *Power Systems in Emergencies: From Contingency Planning to Crisis Management*. Wiley, 2001. [Online]. Available: `https://books.google.se/books?id=sepSAAAAMAAJ`.

[59] D. Aguilar-Dominguez, J. Ejeh, S. F. Brown, and A. D. Dunbar, "Exploring the possibility to provide black start services by using vehicle-to-grid," *Energy Reports*, vol. 8, pp. 74–82, 2022, Multi-CDT Conference in Clean Energy and Sustainable Infrastructure. [Online]. Available: `https://www.sciencedirect.com/science/article/pii/S2352484722012537`.

[60] C. Liu, K. T. Chau, D. Wu, and S. Gao, "Opportunities and Challenges of Vehicle-to-Home, Vehicle-to-Vehicle, and Vehicle-to-Grid Technologies," *Proceedings of the IEEE*, vol. 101, no. 11, pp. 2409–2430, 2013.

[61] S. Vadi, R. Bayindir, A. M. Colak, and E. Hossain, "A review on communication standards and charging topologies of V2G and V2H operation strategies," *Energies*, vol. 12, no. 19, 2019.

[62] S. Zhang, S. Byrne, L. Fennelly, D. Sood, J. O'Donnell, and T. O'Donnell, "Home energy optimization using vehicle-to-home," *Open Research Europe*, vol. 5, no. 48, p. 48, 2025.

[63] B. Zafar and S. A. Ben Slama, "PV-EV integrated home energy management using vehicle-to-home (V2H) technology and household occupant behaviors," *Energy Strategy Reviews*, vol. 44, p. 101 001, 2022.

[64] L. Zhao and V. Aravinthan, "Strategies of residential peak shaving with integration of demand response and V2H," in *2013 IEEE PES Asia-Pacific Power and Energy Engineering Conference (APPEEC)*, IEEE, 2013, pp. 1–5.

[65] D. P. Tuttle, R. L. Fares, R. Baldick, and M. E. Webber, "Plug-In Vehicle to Home (V2H) duration and power output capability," in *2013 IEEE Transportation Electrification Conference and Expo (ITEC)*, 2013, pp. 1–7.

[66] H. Shin and R. Baldick, "Plug-in electric vehicle to home (v2h) operation under a grid outage," *IEEE Transactions on Smart Grid*, vol. 8, no. 4, pp. 2032–2041, 2017.

[67] D. Borge-Diez, D. Icaza, E. Açıkkalp, and H. Amaris, "Combined vehicle to building (V2B) and vehicle to home (V2H) strategy to increase electric vehicle market share," *Energy*, vol. 237, p. 121 608, 2021.

[68] A. Ouammi, "Peak load reduction with a solar PV-based smart microgrid and vehicle-to-building (V2B) concept," *Sustainable Energy Technologies and Assessments*, vol. 44, p. 101 027, 2021.

[69] S. Tian, G. Razeghi, and S. Samuelsen, "Assessment of vehicle-to-load in support of home appliances," *Journal of Energy Storage*, vol. 104, p. 114 406, 2024.

[70] T. J. C. Sousa, L. Machado, D. Pedrosa, C. Martins, V. Monteiro, and J. L. Afonso, "Comparative Analysis of Vehicle-to-Vehicle (V2V) Power Transfer Configurations without Additional Power Converters," in *2020 IEEE 14th International Conference on Compatibility, Power Electronics and Power Engineering (CPE-POWERENG)*, vol. 1, 2020, pp. 88–93.

[71] S. Bhoir, P. Caliandro, and C. Brivio, "Impact of v2g service provision on battery life," *Journal of Energy Storage*, vol. 44, p. 103 178, 2021. [Online]. Available: `https://www.sciencedirect.com/science/article/pii/S2352152X21008781`.

[72] M. A. Razzaque, S. K. Khadem, S. Patra, G. Okwata, and M. Noor-A-Rahim, "Cybersecurity in vehicle-to-grid (V2G) systems: A systematic review," *Applied Energy*, vol. 398, p. 126 364, 2025. [Online]. Available: `https://www.sciencedirect.com/science/article/pii/S0306261925010943`.

[73] J.-M. Tarascon and M. Armand, "Issues and challenges facing rechargeable lithium batteries," *nature*, vol. 414, no. 6861, pp. 359–367, 2001.

[74] R. Xiong, *Battery Management Algorithm for Electric Vehicles*, 1st ed. Springer Singapore, 2020.

[75] G. Zubi, R. Dufo-López, M. Carvalho, and G. Pasaoglu, "The lithium-ion battery: State of the art and future perspectives," *Renewable and sustainable energy reviews*, vol. 89, pp. 292–308, 2018.

[76] N. Nitta, F. Wu, J. T. Lee, and G. Yushin, "Li-ion battery materials: Present and future," *Materials today*, vol. 18, no. 5, pp. 252–264, 2015.

[77] C. R. Birkl, M. R. Roberts, E. McTurk, P. G. Bruce, and D. A. Howey, "Degradation diagnostics for lithium ion cells," *Journal of Power Sources*, vol. 341, pp. 373–386, 2017.

[78] Z. Wu, C. Zhang, F. Yuan, M. Lyu, P. Yang, L. Zhang, M. Zhou, L. Wang, S. Zhang, and L. Wang, "Ni-rich cathode materials for stable high-energy lithium-ion batteries," *Nano Energy*, vol. 126, p. 109 620, 2024. [Online]. Available: `https://www.sciencedirect.com/science/article/pii/S2211285524003689`.

[79] S. Dutta and J. Bauman, "An overview of 800 v passenger electric vehicle onboard chargers: Challenges, topologies, and control," *IEEE Access*, vol. 12, pp. 105 850–105 864, 2024.

[80] J. Vetter, P. Novák, M. Wagner, C. Veit, K.-C. Möller, J. Besenhard, M. Winter, M. Wohlfahrt-Mehrens, C. Vogler, and A. Hammouche, "Ageing mechanisms in lithium-ion batteries," *Journal of Power Sources*, vol. 147, no. 1, pp. 269–281, 2005. [Online]. Available: https://www.sciencedirect.com/science/article/pii/S0378775305000832.

[81] T. Waldmann, B.-I. Hogg, and M. Wohlfahrt-Mehrens, "Li plating as unwanted side reaction in commercial li-ion cells – a review," *Journal of Power Sources*, vol. 384, pp. 107–124, 2018. [Online]. Available: https://www.sciencedirect.com/science/article/pii/S0378775318301848.

[82] Y. Li, D.-I. Stroe, Y. Cheng, H. Sheng, X. Sui, and R. Teodorescu, "On the feature selection for battery state of health estimation based on charging–discharging profiles," *Journal of Energy Storage*, vol. 33, p. 102 122, 2021. [Online]. Available: https://www.sciencedirect.com/science/article/pii/S2352152X20319502.

[83] E. Schaltz, D.-I. Stroe, K. Nørregaard, L. S. Ingvardsen, and A. Christensen, "Incremental capacity analysis applied on electric vehicles for battery state-of-health estimation," *IEEE Transactions on Industry Applications*, vol. 57, no. 2, pp. 1810–1817, 2021.

[84] J. Peng, J. Meng, D. Chen, H. Liu, S. Hao, X. Sui, and X. Du, "A review of lithium-ion battery capacity estimation methods for onboard battery management systems: Recent progress and perspectives," *Batteries*, vol. 8, no. 11, p. 229, 2022.

[85] M. Schimpe, M. E. von Kuepach, M. Naumann, H. C. Hesse, K. Smith, and A. Jossen, "Comprehensive modeling of temperature-dependent degradation mechanisms in lithium iron phosphate batteries," *Journal of The Electrochemical Society*, vol. 165, no. 2, A181, Jan. 2018. [Online]. Available: https://doi.org/10.1149/2.1181714jes.

[86] M. Berecibar, I. Gandiaga, I. Villarreal, N. Omar, J. Van Mierlo, and P. Van den Bossche, "Critical review of state of health estimation methods of li-ion batteries for real applications," *Renewable and Sustainable Energy Reviews*, vol. 56, pp. 572–587, 2016.

[87] M. Naumann, M. Schimpe, P. Keil, H. C. Hesse, and A. Jossen, "Analysis and modeling of calendar aging of a commercial lifepo4/graphite cell," *Journal of Energy Storage*, vol. 17, pp. 153–169, 2018.

[88] C. Xu, P. Behrens, P. Gasper, K. Smith, M. Hu, A. Tukker, and B. Steubing, "Electric vehicle batteries alone could satisfy short-term grid storage demand by as early as 2030," *Nature Communications*, vol. 14, no. 1, p. 119, 2023.

[89] Y. Huang, T. Wik, D. Finegan, Y. Li, and C. Zou, "Learning chemical potentials and parameters from voltage data for multi-phase battery modeling," 2025.

[90] F. Brosa Planella, W. Ai, A. M. Boyce, A. Ghosh, I. Korotkin, S. Sahu, V. Sulzer, R. Timms, T. G. Tranter, M. Zyskin, et al., "A continuum of physics-based lithium-ion battery models reviewed," *Progress in Energy*, vol. 4, no. 4, p. 042 003, 2022.

[91] H. Tu, S. Moura, Y. Wang, and H. Fang, "Integrating physics-based modeling with machine learning for lithium-ion batteries," *Applied energy*, vol. 329, p. 120 289, 2023.

[92] Y. Li, D. Karunathilake, D. M. Vilathgamuwa, Y. Mishra, T. W. Farrell, S. S. Choi, and C. Zou, "Model order reduction techniques for physics-based lithium-ion battery management: A survey," *IEEE Industrial Electronics Magazine*, vol. 16, no. 3, pp. 36–51, 2021.

[93] M. Doyle, T. F. Fuller, and J. Newman, "Modeling of galvanostatic charge and discharge of the lithium/polymer/insertion cell," *Journal of The Electrochemical Society*, vol. 140, no. 6, pp. 1526–1533, 1993.

[94] M. B. Pinson and M. Z. Bazant, "Theory of SEI formation in rechargeable batteries: Capacity fade, accelerated aging and lifetime prediction," *Journal of the Electrochemical Society*, vol. 160, no. 2, A243, 2012.

[95] G. L. Plett, *Battery management systems, Volume II: Equivalent-circuit methods.* Artech House, 2015.

[96] P. Lozano Ruiz, N. Damianakis, and G. Ram Chandra Mouli, "Physics-based and data-driven modeling of degradation mechanisms for lithium-ion batteries—a review," *IEEE Access*, vol. 13, pp. 21 164–21 189, 2025.

[97] S. Li, H. He, C. Su, and P. Zhao, "Data driven battery modeling and management method with aging phenomenon considered," *Applied Energy*, vol. 275, p. 115 340, 2020.

[98] R. Kataoka, A. Shichi, H. Yamada, Y. Iwafune, and K. Ogimoto, "Comparison of the economic and environmental performance of v2h and residential stationary battery: Development of a multi-objective optimization method for homes of ev owners," *World Electric Vehicle Journal*, vol. 10, no. 4, 2019, ISSN: 2032-6653. [Online]. Available: https://www.mdpi.com/2032-6653/10/4/78.

[99] G. Azarbakhsh, A. Mahmoudi, S. Kahourzade, A. Yazdani, and A. Mahmud, "Optimal sizing of photovoltaic and battery energy storage for residential houses in south australia by considering vehicle-to-home operation," *IET Renewable Power Generation*, vol. 19, no. 1, e70053, 2025. [Online]. Available: https://ietresearch.onlinelibrary.wiley.com/doi/abs/10.1049/rpg2.70053.

[100] S. Merrington, R. Khezri, and A. Mahmoudi, "Optimal sizing of grid-connected rooftop photovoltaic and battery energy storage for houses with electric vehicle," *IET Smart Grid*, vol. 6, no. 3, pp. 297–311, 2023. [Online]. Available: https://ietresearch.onlinelibrary.wiley.com/doi/abs/10.1049/stg2.12099.

[101] B. Marion, J. Adelstein, K. e. Boyle, H. Hayden, B. Hammond, T. Fletcher, B. Canada, D. Narang, A. Kimber, L. Mitchell, et al., "Performance parameters for grid-connected pv systems," in *Conference Record of the Thirty-first IEEE Photovoltaic Specialists Conference, 2005.*, IEEE, 2005, pp. 1601–1606.

[102] J. Lindahl, "National survey report of pv power applications in sweden 2010," IEA Photovoltaic Power Systems Programme (IEA-PVPS), Task 1, Tech. Rep., May 2011, Prepared for the IEA PV Power Systems Programme; funded by the Swedish Energy Agency. Document date: 2011-05-20. [Online]. Available: https://iea-pvps.org/wp-content/uploads/2020/01/nsr_2010_SWE.pdf.

[103] D. Rayner, F. Lindberg, J. Kukulies, S. Thorsson, and N. Wallenberg, *Urban climate data for Gothenburg, 1983-2020*, en, 2021. [Online]. Available: https://doi.org/10.5878/a2h2-4s63.

[104] B. Smith, M. Woodhouse, K. Horowitz, T. Silverman, J. Zuboy, and R. Margolis, "Photovoltaic (PV) Module Technologies: 2020 Benchmark Costs and Technology Evolution Framework Results," National Renewable Energy Laboratory (NREL), Tech. Rep., 2021, Benchmark assumptions include 400-W modules.

[105] C. Hamzaçebi, D. Akay, and F. Kutay, "Comparison of direct and iterative artificial neural network forecast approaches in multi-periodic time series forecasting," *Expert Systems with Applications*, vol. 36, no. 2, pp. 3839–3844, 2009.

[106] National Renewable Energy Laboratory (NREL), *End-use load profiles for the U.S. building stock [data set]*, 2021. [Online]. Available: `https://data.openei.org/submissions/4520`.

[107] L. Breiman, "Random forests," *Machine learning*, vol. 45, no. 1, pp. 5–32, 2001.

[108] T. M. Mitchell, "Does machine learning really work?" *AI magazine*, vol. 18, no. 3, pp. 11–11, 1997.

[109] C. M. Bishop, *Pattern Recognition and Machine Learning* (Information Science and Statistics). New York, NY: Springer, 2006.

[110] I. Goodfellow, Y. Bengio, and A. Courville, *Deep Learning*. Cambridge, MA: MIT Press, 2016, `http://www.deeplearningbook.org`.

[111] Y. LeCun, Y. Bengio, and G. Hinton, "Deep learning," *Nature*, vol. 521, no. 7553, pp. 436–444, 2015. [Online]. Available: `https://doi.org/10.1038/nature14539`.

[112] R. J. Hyndman and G. Athanasopoulos, *Forecasting: Principles and Practice*, 3rd ed. OTexts, 2021. [Online]. Available: `https://otexts.com/fpp3/`.

[113] K. Benidis, S. S. Rangapuram, V. Flunkert, B. Wang, D. C. Maddix, C. Turkmen, J. Gasthaus, M. Bohlke-Schneider, D. Salinas, L. Stella, et al., "Neural forecasting: Introduction and literature overview," *arXiv preprint arXiv:2004.10240*, 2020. [Online]. Available: `https://arxiv.org/abs/2004.10240`.

[114] S. Hochreiter and J. Schmidhuber, "Long short-term memory," *Neural Computation*, vol. 9, no. 8, pp. 1735–1780, 1997.

[115] A. Vaswani, N. Shazeer, N. Parmar, J. Uszkoreit, L. Jones, A. N. Gomez, Ł. Kaiser, and I. Polosukhin, "Attention is all you need," in *Advances in Neural Information Processing Systems (NeurIPS)*, vol. 30, 2017.

[116] Y. Bengio, P. Simard, and P. Frasconi, "Learning long-term dependencies with gradient descent is difficult," *IEEE transactions on neural networks*, vol. 5, no. 2, pp. 157–166, 1994.

[117] N. Lu, Q. Ouyang, Y. Li, and C. Zou, "Electrical load forecasting model using hybrid LSTM neural networks with online correction," *arXiv preprint arXiv:2403.03898*, 2024.

[118] U. Hussan, H. Wang, J. Peng, H. Jiang, and H. Rasheed, "Transformer-based renewable energy forecasting: A comprehensive review," *Renewable and Sustainable Energy Reviews*, vol. 226, p. 116 356, 2026, ISSN: 1364-0321.

[119] C. Park, *Fundamentals of Engineering Economics*. Upper Saddle River, NJ, USA: Pearson Education, 2013.

[120] A. Esmaeel Nezhad, A. Rahimnejad, P. H. J. Nardelli, S. A. Gadsden, S. Sahoo, and F. Ghanavati, "A shrinking horizon model predictive controller for daily scheduling of home energy management systems," *IEEE Access*, vol. 10, pp. 29 716–29 730, 2022.

[121] G. H. Danielsson, L. N. F. da Silva, J. L. da Paixão, A. d. R. Abaide, and N. K. Neto, "Rules-based energy management system for an ev charging station nanogrid: A stochastic analysis," *Energies*, vol. 18, no. 1, p. 26, 2024.

[122] D. Q. Mayne, M. M. Seron, and S. V. Raković, "Robust model predictive control of constrained linear systems with bounded disturbances," *Automatica*, vol. 41, no. 2, pp. 219–224, 2005.

[123] A. Mesbah, "Stochastic model predictive control: An overview and perspectives for future research," *IEEE Control Systems Magazine*, vol. 36, no. 6, pp. 30–44, 2016.

[124] R. S. Sutton and A. G. Barto, *Reinforcement Learning: An Introduction*, 2nd ed. The MIT Press, 2018.

[125] H. T. Dinh, D. Kim, and D. Kim, "MILP-based optimal day-ahead scheduling for a system-centric community energy management system supporting different types of homes and energy trading," *Scientific Reports*, vol. 12, p. 17 359, 2022.

[126] N. Fesakis, C. Megagiannis, G. E. Lazaridou, E. Sarafoglou, A. Tzouvaras, and A. Karlis, "Energy management in multi-source electric vehicles through multi-objective whale particle swarm optimization considering aging effects," *Energies*, vol. 19, no. 1, 2026. [Online]. Available: `https://www.mdpi.com/1996-1073/19/1/154`.